

**Green Synthesis of Fe-doped zinc oxide Nanoparticle for Removal of Methylene blue dye
from Aqueous Solution**



Wondimlebesku Delelegn Haile

**A Thesis Study submitted to department of applied chemistry in partial fulfilment of the
requirements for masters of Science in applied chemistry**

College of Natural and Computational Science

Postgraduate studies

Wolkite University

January 10 2025 GC

Wolkite, Ethiopia

**Green Synthesis of Fe-doped zinc oxide Nanoparticle for Removal of Methylene blue dye
from Aqueous Solution**

Wondimlebesku Delelegn Haile

Advisor; - Dr. Israel Leka (PhD)

**A Thesis Submitted to the Department of Applied Chemistry,
College of Natural and Computational Sciences Office of Graduate Studies**

Wolkite University

Januar2025G.C.

Wolkite, Ethiopia

Declaration

I hereby declare that this Master Thesis entitled “**Green synthesis of Fe-doped Zinc Oxide nanoparticle for removal of methylene blue dye from aqueous solution**” is my original work. That is, it has not been submitted for the award of any academic degree, diploma, or certificate in any other university. All sources of materials that are used for this thesis have been duly acknowledged through citation.

Name of Student

Signature

Date

Acknowledgement

First and foremost, I would like to express my heartfelt gratitude to the Almighty God and to His blessed mother, St. Mary, for bestowing upon me the health, strength, wisdom, and patience necessary to successfully complete this thesis. Without their divine guidance, I would not have had the perseverance to overcome the challenges encountered throughout this journey.

I am deeply indebted to my advisor, Dr. Israel Leka (PhD), whose invaluable guidance and support have been instrumental in the successful completion of this work. His insightful suggestions, constructive criticisms, and tireless supervision provided me with the direction and motivation needed to carry out this research. I am particularly grateful for the fatherly consultation he extended to me throughout the process, offering both academic and personal support. His commitment to reviewing and refining my document from the initial proposal stage to the final thesis submission has been essential to my success.

I am deeply indebted to my Co-advisor, Dr. Teshale Assefa (PhD), whose invaluable guidance and support have been instrumental in the successful completion of this work. His insightful suggestions, constructive criticisms, and tireless supervision provided me with the direction and motivation needed to carry out this research.

I would also like to extend my profound appreciation to my family, whose unwavering support—both financially and morally—has been a source of strength and encouragement. Their belief in me, especially during difficult times, has kept me focused and motivated to push forward and complete my work. I am grateful for their patience and understanding throughout this endeavor. A special thanks goes to my colleagues and the Chemistry Laboratory Technicians. Furthermore, I would like to extend my sincere thanks to Wolkite University's Chemistry Department for providing me access to the UV-Vis spectrometer, which was critical for the adsorption experiments conducted as part of my research. I am equally grateful to Addis Ababa Science and Technology University's Central Laboratory for facilitating my access to their FT-IR, XRD, and UV-DRS analytical instruments, without which crucial data for this thesis would have been difficult to obtain. Lastly, I am thankful to all those who, in one way or another, contributed to the completion of this research. Their support, whether through intellectual input, technical assistance, or moral encouragement, has been deeply appreciated.

Contents	Pages
Declaration.....	iii
Recommendation	iv
Approval Sheet.....	v
LIST OF TABLE	x
LIST OF FIGURE.....	xi
LIST OF ABBREVIATION.....	xii
Abstract.....	xiii
CHAPTER ONE	1
1 INTRODUCTION	1
1.1 Background of the study	1
1.2 Statement of problem.....	3
1.3 Objectives of the study.....	5
1.3.1 General objective of the study.....	5
1.3.2 Specific objective of the study	5
1.4 Significance of the Study	5
1.5 The scope of the study	6
CHAPTER TWO	9
2.LITERATURE REVIEW	9
2.1 Dye Contamination in Water Bodies	9
2.2 Traditional Methods for Dye Removal	9
2.3 Adsorption as a Technique for Dye Removal	10
2.4 Zinc Oxide (ZnO) Nanoparticles for Dye Removal.....	10
2.5 Enhancement of ZnO Properties by Doping with Iron (Fe).....	10
2.6 Green Synthesis of Metal Oxide Nanoparticles	11
2.7 Applications of Fe-doped ZnO Nanoparticles in Dye Removal	11
2.8 Adsorption Mechanism of Methylene Blue on the Surface of Fe-Doped ZnO Nanoparticles	12
2.8.1 Surface Characteristics of Fe-Doped ZnO Nanoparticles	12
2.8.2. Electrostatic Interactions	12
2.8.3 Surface Complexation and Hydrogen Bonding	13
2.8.4 Photocatalytic Effect (If Applicable).....	13
2.8.5 Adsorption Isotherms	13
2.8.6 Kinetics of Adsorption	14
2.8.7 Regeneration and Reusability	14
2.9 Knowledge Gaps and Research Opportunities.....	15

CHAPTER THREE	16
3 MATERIAL AND METHODS	16
3.1 Apparatus and Instruments.....	16
3.2 Chemical and reagents	16
3.3 Experimental site	16
3.4 Methods and Procedures	16
3.4.1 Collection of justicia Adhatoda Plant Leaf	16
3.4.2 Preparation of Justicia adhatoda Leaf Extract	17
3.4.3 Preparation of Undoped zinc oxide	17
3.4.4 Preparation of Fe-doped ZnO nanoparticles	17
3.5 Characterization studies	18
3.6 Removal of Methylene blue using Fe-doped zinc oxide nanoparticle by sorption	18
3.6.1 Preparation of working standard solutions	18
3.6.2 Batch sorption experiment	18
3.6.3 Sorption kinetic studies.....	19
3.6.4 Reusability test of Fe-doped zinc oxide nanoparticles	19
CHAPTER FOUR.....	20
4.RESULT AND DISCUSSION	20
4.1 Characterization of synthesized adsorbent.....	20
4.1.1 UV-Vis DRS Analysis of ZnO and Fe-ZnO NPs	20
4.1.2 XRD analysis of ZnO and Fe-ZnO NPs.....	21
4.1.3 FTIR Analysis of ZnO, Fe-ZnO and Plant extract.....	23
4.2 Optimization of adsorbent for removal of MB dye from aqueous solution	24
4.2.1 Calibration plot of working methylene blue standard solution.....	24
4.3 MB dye adsorption by using ZnO and Fe doped ZnO NPs	26
4.3.1 Effect of pH on the Adsorption of Methylene Blue Dye	26
4.3.2 Effect of Adsorbent Dosage on the Adsorption of Methylene Blue Dye	27
4.3.3 Effect of Contact Time on the Adsorption of Methylene Blue Dye	29
4.3.4 Effect of initial concentration	32
4.3.5 Reusability test of Fe doped ZnO NPs.....	33
4.5 Adsorption kinetics Study	35
4.4.1 Pseudo-first order kinetics.....	36
4.4.2 Pseudo-second order kinetics.....	36

CHAPTER FIVE	40
5. CONCLUSION AND RECOMMENDATION	40
5.1 Conclusion	40
5.2 Recommendation	41
REFERENCES	42
APPENDIX.....	49

LIST OF TABLE

Table	Pages
Table 1: Expected oxidation and charge state of Mn and Fe ions presented in ZnO	13
Table 2: Methylene blue dye working standard solution calibration data	24
Table 3: Parameters of pseudo-1 st order and pseudo-2 nd order for synthesized samples	31

LIST OF FIGURE

Figure	Pages
Figure 1: (a) Ferromagnetic DMS, an alloy between nonmagnetic semiconductor and TM and (b) anti ferromagnetic DMS.	12
Figure 2: Electronic configuration of 3d-states and 4s-states of TMs.	12
Figure 3: chemical structure of methylene blue	15
Figure 4: UV-DRS spectrum of ZnO and Fe-ZnO NPs	21
Figure 5: XRD spectrum of ZnO and Fe doped ZnO NPs	22
Figure 6: FTIR spectra of ZnO, Fe doped ZnO and Plant extract	24
Figure 7: Calibration plot of working MB standards solution	25
Figure 8: Effect of pH on MB dye removal	26
Figure 9: Effect of adsorbent dose on MB dye removal	26
Figure 10: Effect of contact time on MB dye removal	27
Figure 11: Effect of initial concentration on MB dye removal	28
Figure 12: Reusability test of Fe-ZnO NPs adsorbent for the removal of methylene blue dye.	29
Figure 13: pseudo second-order models of (a) ZnO NPs, (b) Fe-ZnO NPs.	30

LIST OF ABBREVIATION

AOPS	Advanced Oxidation Process
E _g	Bandgap Energy
BET	Brunauer–Emmett–Teller
CB	Conduction band
DTA	Differential thermal analysis
DRS	Diffuse reflectance spectra
eV	Electron volt
FTIR	Fourier Transform Infrared
JCPDS	Joint Committee on Powder Diffraction Standards
MB	Methylene Blue
MO	Methyl orange
MG	Methyl green
NPs	Nanoparticles
PL	Photoluminescence
SEM	Scanning electron Microscopy
TGA	Thermo Gravimetric Analysis
TEM	Transmission electron Microscopy
UV-Vis	Ultra Violet Visible
VB	Valence band
XRD	X-ray Powder Diffraction

Abstract

In this study, Zinc oxide (ZnO) and iron-doped zinc oxide (Fe-doped ZnO) nanoparticles were synthesized using a green sol–gel method, utilizing *Justicia Adhatoda* plant leaf extract as a reducing agent. The aim was to investigate the potential of these nanoparticles as adsorbents for the removal of methylene blue dye, a toxic effluent commonly found in wastewater from textile industries. The synthesized materials were thoroughly characterized using various techniques: X-ray diffraction (XRD), Fourier transform infrared spectroscopy (FT-IR), and UV-visible (UV-VIS) spectroscopy.

XRD analysis confirmed that both ZnO and Fe-doped ZnO nanoparticles exhibited a hexagonal wurtzite crystal structure, with good crystallinity and phase purity. The average particle sizes were found to be 24 nm for pure ZnO and 20 nm for Fe-doped ZnO, indicating that doping with iron slightly reduced the particle size. FT-IR analysis revealed key absorbance peaks corresponding to functional groups from the plant extract, confirming the involvement of the plant's organic compounds in the nanoparticle synthesis. The UV-VIS results showed a shift in the absorption spectra of Fe-doped ZnO nanoparticles, with the maximum absorption wavelength moving from the ultraviolet (UV) region to the visible range, indicating enhanced optical properties due to iron doping. The adsorption performance of the ZnO and Fe-doped ZnO nanoparticles was evaluated under various conditions. The optimum removal efficiency for ZnO nanoparticles was achieved at pH 9, with an adsorbent dose of 20 mg, a contact time of 45 minutes, and an initial dye concentration of 5 mg/L, resulting in a dye removal efficiency of 95.23%. For Fe-doped ZnO nanoparticles, the same conditions led to a higher removal efficiency of 99.52%. The adsorption kinetics followed the pseudo-second-order model, suggesting chemisorption as the primary mechanism of dye removal. Furthermore, the study demonstrated the recyclability of the synthesized nanocomposites, showing that they could be effectively used for more than five cycles without significant loss in efficiency. These findings suggest that the green-synthesized ZnO and Fe-doped ZnO nanoparticles are promising, eco-friendly adsorbent materials for wastewater treatment, particularly for removing hazardous dyes like methylene blue, and could be applied in sustainable, cyclic water purification processes.

Keywords: adsorbent, *Justicia adhatoda*, green synthesis, nanoparticles, optimization, Fe-doped ZnO.

CHAPTER ONE

1 INTRODUCTION

1.1 Background of the study

Water pollution, particularly through the discharge of industrial effluents, is one of the most pressing environmental challenges facing the world today. Among the various industries contributing to water contamination, textile industries are major culprits due to the large volumes of water they consume and the chemicals they release. A significant concern within textile wastewater is the presence of synthetic dyes, especially methylene blue (MB). Methylene blue is a commonly used cationic dye in textiles, but its environmental impact is substantial. If not properly treated, MB can persist in water systems, accumulating in aquatic environments and potentially harming ecosystems. It is toxic to aquatic organisms, disrupts photosynthetic processes, and can bioaccumulate in the food chain, leading to detrimental effects on human health through consumption of contaminated water or food. Given its toxicity and persistence, the effective removal of methylene blue from wastewater has become a critical area of research in environmental engineering. Several methods have been explored for this purpose, including chemical, biological, and physical processes. Among these, adsorption has gained considerable attention as one of the most effective, economical, and versatile techniques for removing organic pollutants, such as methylene blue, from aqueous solutions. Adsorption involves the attachment of pollutants onto the surface of an adsorbent material, and it is particularly useful for the removal of dyes due to the large surface area and high adsorption capacity of certain materials. In the search for effective adsorbents, metal oxide nanoparticles have emerged as promising candidates. Among these, Zinc oxide (ZnO) nanoparticles have garnered significant interest due to their high surface area, stability, and photocatalytic properties. ZnO is a semiconductor material that has been widely researched for its potential applications in environmental remediation, particularly in the removal of dyes. When exposed to ultraviolet (UV) light, ZnO nanoparticles can both adsorb and degrade organic pollutants through photocatalytic reactions, making them highly effective for wastewater treatment. However, while pure ZnO nanoparticles show promise, they have limitations. Their adsorption capacity can be affected by factors such as pH, the presence of other ions, and the nature of the dye itself. Furthermore, their photocatalytic activity is primarily active under UV light, which limits their effectiveness under natural light conditions.

To overcome these limitations, doping ZnO with transition metals, such as iron (Fe), has been proposed. Iron-doped ZnO nanoparticles (Fe-doped ZnO) exhibit enhanced photocatalytic activity, improved stability, and greater adsorption capacity compared to pure ZnO. The introduction of iron ions into the ZnO lattice creates defect sites that can serve as active centers for pollutant adsorption. These defect sites also play a key role in enhancing the material's photocatalytic properties, as the iron dopants narrow the band gap of ZnO, allowing it to absorb light in the visible region as well as the UV region. This shift to visible light absorption makes Fe-doped ZnO more effective under natural sunlight, thereby improving its utility in real-world applications. Additionally, iron doping can increase the stability and recyclability of ZnO nanoparticles, making them a more sustainable option for long-term use in wastewater treatment. While doping ZnO with iron offers numerous advantages, the synthesis of these nanoparticles typically requires the use of chemical reducing agents, which can be hazardous to both human health and the environment. In recent years, there has been a growing shift towards green synthesis methods, which employ natural, non-toxic materials to produce nanoparticles. Green synthesis methods are attractive because they avoid the use of toxic chemicals, require milder reaction conditions, and are more environmentally friendly. Plant extracts, in particular, have gained prominence as reducing and stabilizing agents in the synthesis of metal oxide nanoparticles. Plants contain a variety of bioactive compounds, such as flavonoids, alkaloids, tannins, and other phenolic compounds, that can act as reducing agents to convert metal ions into nanoparticles. *Justicia adhatoda*, a medicinal plant known for its pharmacological properties, is one such plant that has shown great potential for the green synthesis of nanoparticles. The plant is rich in bioactive compounds such as alkaloids (e.g., vasicine), flavonoids, and tannins, which have strong antioxidant and reducing properties. These compounds make *Justicia adhatoda* an ideal candidate for the green synthesis of metal oxide nanoparticles, including ZnO and Fe-doped ZnO. By using *Justicia adhatoda* leaf extract as a reducing agent, it is possible to create nanoparticles that are not only environmentally friendly but may also possess additional functional properties derived from the plant's bioactive compounds.

The use of *Justicia Adhatoda* extract for the synthesis of Fe-doped ZnO nanoparticles aligns well with the principles of green chemistry, offering a sustainable and eco-friendly alternative to traditional synthetic methods. The phytochemicals in the leaf extract can help stabilize the nanoparticles, preventing agglomeration and ensuring their uniform dispersion. This stabilization is crucial for enhancing the material's surface area and adsorption capacity. Furthermore, the

bioactive compounds in the plant extract may also contribute to the photocatalytic and adsorptive properties of the nanoparticles, potentially improving their performance in dye removal applications.

1.2 Statement of problem

Water pollution, particularly the contamination of aquatic ecosystems by industrial effluents, is a significant environmental issue. Among the various pollutants discharged into water bodies, synthetic dyes especially those used in the textile industry pose a serious threat. Methylene blue (MB), a commonly used cationic dye in textile processing, is particularly concerning due to its toxic effects on both aquatic life and human health. It is highly persistent in the environment, making it difficult to degrade using conventional waste water treatment methods. The accumulation of methylene blue in water sources leads to contamination of drinking water and disruption of ecosystems, making its effective removal from wastewater a critical environmental challenge. Traditional methods for dye removal, such as chemical coagulation, filtration, and biological treatments, are of time efficient, costly, or environmentally damaging. In response to these challenges, adsorption has emerged as a promising, cost effective, and efficient technique for removing dyes from aqueous solutions. Among various adsorbent materials, metal oxide nano particles, particularly Zinc oxide (ZnO), have gained attention due to their high surface area, stability, and photocatalytic properties. However, the adsorption efficiency of pure ZnO nanoparticles is often limited by factors such as their photocatalytic activity under UV light and their adsorption capacity in the presence of competing ions or varying environmental conditions. Iron doped Zinc oxide nano particles (Fe doped ZnO) have shown improved adsorption properties, as the incorporation of iron into the ZnO lattice created defect sites and narrows the material's band gap, enhancing its efficiency under visible light. This modification increases both the photocatalytic activity and adsorption capacity of ZnO, making Fe-doped ZnO a more effective candidate for dye removal. However, the synthesis of these nano particles typically involves chemical reagents that may be harmful to the environment. In recent years, green synthesis methods using natural substances such as plant extracts have gained attention as environmentally friendly alternatives to traditional chemical approaches. *Justicia adhatoda*, a plant known for its medicinal properties and rich in bioactive compounds such as flavonoids and alkaloids, has demonstrated potential as a reducing agent in the synthesis of metal oxide nano particles. Using *Justicia adhatoda* leaf extract for the green synthesis of Fe-doped ZnO nanoparticles is a sustainable and eco-friendly approach,

while also potentially enhancing the nanoparticles' adsorptive and photocatalytic properties due to the plant's inherent bioactive compounds. Despite the promising potential of Fe-doped ZnO nanoparticles synthesized through green methods, there remains a significant gap in understanding their effectiveness and practical application in removing toxic dyes such as methylene blue. The challenge lies in optimizing synthesis conditions to produce nanoparticles with high surface area, stability, and reusability, and in evaluating their performance in real-world scenarios, particularly in removing methylene blue from aqueous solutions under various environmental conditions. Therefore, the problem this study aims to address is the need for an environmentally friendly and effective method for synthesizing iron-doped zinc oxide nanoparticles using *Justicia adhatoda* leaf extract, and evaluating their potential as adsorbents for the removal of methylene blue dye from aqueous solutions. By exploring the synthesis, characterization, and dye removal efficiency of these nanoparticles, this research seeks to contribute to the development of sustainable, green nano materials for effective wastewater treatment.

Metal oxide nano particles. Using *Justicia adhatoda* leaf extract for the green synthesis of Fe-doped ZnO nanoparticles of for sustainable and eco-friendly approach, while also potentially enhancing the nanoparticles' adsorptive and photocatalytic properties due to the plant's inherent bioactive compounds. Despite the promising potential of Fe-doped ZnO nanoparticles synthesized through green methods, there remains a significant gap in understanding their effectiveness and practical application in removing toxic dyes such as methylene blue. The challenge lies in optimizing synthesis conditions to produce nanoparticles with high surface area, stability, and reusability, and in evaluating their performance in real-world scenarios, particularly in removing methylene blue from aqueous solutions under various environmental conditions. Therefore, the problem this study aims to address is the need for an environmentally friendly and effective method for synthesizing iron-doped zinc oxide nanoparticles using *Justicia adhatoda* leaf extract, and evaluating their potential as adsorbents for the removal of methylene blue dye from aqueous solutions. By exploring the synthesis, characterization, and dye removal efficiency of these nanoparticles, this research seeks to contribute to the development of sustainable, green nano materials for effective wastewater treatment.

1.3 Objectives of the study

1.3.1 General objective of the study

The general objective of this study were to synthesize and characterize iron-doped zinc oxide (Fe-doped ZnO) nanoparticle using *Justicia adhatoda* leaf extract for removal of methylene blue dye from aqueous solution.

1.3.2 Specific objective of the study

The specific objectives of this study was:-

- ❖ To Synthesize Fe-doped ZnO nanoparticles via a green sol-gel method using the leaf extract of *Justicia adhatoda*
- ❖ To Characterize the synthesized nanoparticles in terms of their structural, optical, and functional properties using techniques such as X-ray diffraction (XRD), Fourier transform infrared spectroscopy (FT-IR), and UV-visible (UV-VIS) spectroscopy
- ❖ To Evaluate the removal efficiency of methylene blue dye from aqueous solutions using the synthesized Fe-doped ZnO nanoparticles, optimizing parameters such as pH, adsorbent dose, contact time, and initial dye concentration
- ❖ To Evaluate the adsorption kinetics and mechanisms, particularly focusing on the interaction between the dye molecules and the nanoparticles, to evaluate their potential for real-world wastewater treatment applications
- ❖ Assess the recyclability and long-term stability of the synthesized nanoparticles to determine their sustainability in repeated use for dye removal.

1.4 Significance of the Study

The significance of this study lies in its potential to contribute to both environmental protection and the development of sustainable materials for waste water treatment. The removal of methylene blue dye from waste water is a growing concern, particularly due to its wide spread use in the textile industry and its toxic impact on aquatic ecosystems and human health. Traditional methods for dye removal, while useful, often face challenges such as in efficiency, high cost, or environmental harm. This study seeks to address these limitations by exploring an eco-friendly, cost-effective, and efficient alternative: the use of iron-doped zinc oxide (Fe-doped ZnO) nanoparticles synthesized through a green method using *Justicia adhatoda* leaf extract. By utilizing plant-based green synthesis, this study emphasizes a more sustainable approach to nanoparticle production, avoiding

the use of hazardous chemicals typically involved in conventional synthesis methods. The use of *Justicia adhatoda*, a plant with known anti oxidant and reducing properties, offers an innovative solution to synthesizing nanoparticles in an environmentally responsible manner. This method not only reduces the environmental impact but also potentially enhances the properties of the resulting nanoparticles, such as improved stability, adsorption capacity, and photocatalytic activity, which are critical for efficient dye removal. The incorporation of iron into the ZnO lattice (Fe-doped ZnO) further enhances the material's effectiveness. Iron doping improves the photocatalytic properties of ZnO, enabling it to work under visible light, which is more practical than UV light for real-world applications. Additionally, the defect sites created by iron doping may lead to better adsorption of methylene blue dye, increasing the efficiency of the removal process. By examining the potential of Fe-doped ZnO nanoparticles synthesized using a natural, green method, this study aims to provide valuable insights into how these materials can be optimized for practical use in the treatment of industrial waste water. Furthermore, the development of a green, recyclable adsorbent material could have broader implications for various applications beyond dye removal, including the remediation of other environmental pollutants. The findings of this study could contribute to the development of cost-effective, sustainable, and scalable solutions for wastewater treatment, addressing both the growing global concern over water pollution and the need for eco-friendly technologies in industrial processes. In general, this study is significant because it explores a novel, sustainable approach to synthesizing Fe-doped ZnO nanoparticles, evaluates their performance in dye removal, and contributes to the broader effort of developing green materials for environmental remediation. The research aligns with current trends toward sustainable nano material synthesis and offers potential applications in both industrial and environmental settings.

1.5 The scope of the study

The scope of this study is focused on the synthesis, characterization, and application of iron-doped zinc oxide (Fe-doped ZnO) nanoparticles for the removal of methylene blue dye from aqueous solutions, using *Justicia adhatoda* leaf extract as a green reducing and stabilizing agent. The study aims to explore and evaluate the following key aspects: Synthesis of Fe-doped ZnO Nanoparticles: The study will investigate the synthesis of iron-doped zinc oxide nanoparticles using a green sol-gel method. *Justicia adhatoda* leaf extract, rich in bioactive compounds, will be used to reduce and stabilize the metal ions during the synthesis process. The iron doping will be varied to optimize the synthesis conditions for achieving the desired nanoparticle properties. Characterization of the

Nanoparticles: The synthesized Fe-doped ZnO nanoparticles will be characterized using various techniques to understand their structural, chemical, and optical properties. X-ray diffraction (XRD) to determine the crystallinity, phase purity, and crystal structure (wurtzite structure) of the nanoparticles. Fourier-transform infrared (FT-IR) spectroscopy to identify functional groups and confirm the presence of organic compounds from the leaf extract that may be involved in the nanoparticle synthesis. UV-visible (UV-VIS) spectroscopy to evaluate the optical properties, including the shift in absorption spectra due to iron doping and the potential photocatalytic activity under different light conditions. Adsorption Studies: The study will evaluate the efficiency of Fe-doped ZnO nanoparticles in removing methylene blue dye from aqueous solutions. This will involve studying the effects of various parameters such as: pH of the solution: To determine the optimum pH for maximum dye removal. Adsorbent dose: To identify the optimal amount of nanoparticles required for effective dye removal. Contact time: To assess how the removal efficiency changes over time. Initial dye concentration: To study the effect of varying dye concentrations on the adsorption process, adsorption kinetics and mechanism. The study will investigate the adsorption kinetics of methylene blue dye on Fe-doped ZnO nanoparticles, specifically evaluating the fit of experimental data to kinetic models such as the pseudo-first-order and pseudo-second-order models.

The adsorption mechanism will also be explored to understand the interaction between the dye molecules and the nanoparticles. Comparison with Pure ZnO Nanoparticles: A comparison will be made between the adsorption performance of Fe-doped ZnO and pure ZnO nanoparticles, allowing for an assessment of the benefits and improvements brought about by iron doping in terms of adsorption efficiency, photocatalytic activity, and overall performance.

1.6 Limitations and Delimitations:

The study was focused solely on the removal of methylene blue dye, and while other dyes may also be removed using Fe-doped ZnO nanoparticles, this study was not explore their removal in detail. The synthesis and characterization will be limited to the sol-gel method using *Justicia adhatoda* leaf extract, and other plant extracts or methods are not within the scope of this study. The study will be conducted under laboratory conditions and does not include testing in real industrial effluent or large-scale settings, which could involve more complex variables. In general, the scope of this study is confined to the green synthesis, characterization, and evaluation of Fe-doped ZnO

nanoparticles for the removal of methylene blue dye, with a focus on optimizing conditions, understanding the adsorption process, and assessing the potential for sustainable, environmentally friendly wastewater treatment applications.

CHAPTER TWO

2.LITERATURE REVIEW

Removing toxic dyes from industrial waste water has become a major environmental issue, especially in the textile industry, which is a major cause of water pollution worldwide. Methylene blue (MB), a cationic dye widely used in the textile industry, is notorious for its persistence in the environment and its toxic effects on aquatic life and human health. In recent years, several methods have been studied to remove dyes from wastewater, with adsorption proving to be one of the most effective and cost-effective methods. This section reviews the literature on the use of nanoparticles, particularly zinc oxide (ZnO) and iron-doped zinc oxide (Fe-doped ZnO), as adsorbents for dye removal, and the growing interest in green synthetic methods, including the use of plant extracts for nanoparticle production

2.1 Dye Contamination in Water Bodies

The textile industry contributes significantly to water pollution by releasing large amounts of dyes and other chemical pollutants into water bodies. Methylene blue, a widely used dye, is one of the most common dyes that contaminate waste water. When released into the environment, MB poses serious risks to aquatic eco systems, causing toxicity to fish, algae, and other aquatic organisms. Moreover, it is resistant to natural degradation processes and remains in water for prolonged periods, making its removal from wastewater a critical concern (Chen et al., 2012; Suresh et al., 2020).

2.2 Traditional Methods for Dye Removal

Removing toxic dyes from industrial waste water has become a major environmental issue, especially in the textile industry, which is a major cause of water pollution worldwide. Methylene blue (MB), a cationic dye widely used in the textile industry, is notorious for its persistence in the environment and its toxic effects on aquatic life and human health. In recent years, several methods have been studied to remove dyes from wastewater, with adsorption proving to be one of the most effective and cost-effective methods. This section reviews the literature on the use of nanoparticles, particularly zinc oxide (ZnO) and iron-doped zinc oxide (Fe-doped ZnO), as adsorbents for dye removal, and the growing interest in green synthetic methods, including the use of plant extracts for nanoparticle production

2.3 Adsorption as a Technique for Dye Removal

Adsorption is a process in which pollutants, such as dyes, are removed from the aqueous solution with their accumulation on the surface of the solid adsorbent. This method is highly effective due to its simplicity, low cost, and ease of operation. Various materials, including activated carbon, clays, polymers, and metal oxides have been studied for their adsorption capacity. Among these materials, metal oxide nanoparticles such as zinc oxide (ZnO) have attracted significant attention because of their large surface area and high chemical stability, along with their photocatalytic properties (Zhao et al., 2013; Li et al., 2015).

2.4 Zinc Oxide (ZnO) Nanoparticles for Dye Removal

ZnO nanoparticles are one of the most widely researched materials to remove contaminants including dyes from water. ZnO is a wide band gap semiconductor material that enables photocatalytic degradation of organic pollutants under UV irradiation. Additionally, its high surface area, combined with its ability to adsorb organic pollutants, makes it an effective material for dye removal. Several studies have demonstrated the effectiveness of ZnO nanoparticles in removing methylene blue from aqueous solutions. (Zhao et al., 2012; Ching et al., 2013). However, ZnO nanoparticles typically require UV light to activate their photocatalytic properties, limiting their performance under natural light conditions. Moreover, the adsorption capacity of pure ZnO nanoparticles can be restricted by factors such as particle aggregation, stability, and reusability (Parida et al., 2015).

2.5 Enhancement of ZnO Properties by Doping with Iron (Fe)

To overcome the limitations of purity, doping with transition metals such as iron (Fe) has been proposed as a method to enhance its photocatalytic and adsorptive properties. Iron-doped ZnO nanoparticles (Fe-doped ZnO) exhibit improved photocatalytic activity and adsorption efficiency due to several factors. The introduction of iron into the ZnO lattice creates defect sites that serve as active centers for pollutant adsorption. Additionally, iron doping narrows the band gap of ZnO, allowing it to absorb visible light, which makes Fe-doped ZnO more effective under natural sunlight compared to pure ZnO (Raut et al., 2013; Ramaraj et al., 2014). Studies have shown that Fe-doped ZnO nanoparticles exhibit higher dye removal efficiency compared to pure ZnO. Switching to pure

ZnO due to increased surface area and improved electronic properties (Chakraborty et al., 2016; Wanget al., 2019).

2.6 Green Synthesis of Metal Oxide Nanoparticles

Traditional methods for synthesizing metal oxide nanoparticles often require the use of toxic chemicals, green synthesis offers a more environmentally friendly alternative. Green synthesis involves the Use of natural substances such as plant extracts, as reducing agents to synthesize nanoparticles. Plant-based synthesis the method is profitable because of its eco-friendly nature, Cost-effective and ability to produce nanoparticles with well-controlled size and shape. In addition, plant extracts contain many bioactive compounds such as poly phenols, flavonoids, and alkaloids, which can act as reducing agents and stabilizers during synthesis. (Vijayakumar et al., 2016; Sangeetha et al., 2020).

Justicia adhatoda, a medicinal plant known for its bioactive compounds, has been studied for its potential in green synthesis of metal oxide nanoparticles, plants contain alkaloids, flavonoids and tannins with strong antioxidant effects and reducing properties. Several studies have shown that *Justicia adhatoda* leaf extract can effectively reduce metal salt to form metal oxide nanoparticles, including zinc oxide (ZnO) and its doped forms (Srinivasan et al., 2015). The use of *Justicia adhatoda* leaf extract for synthesizing iron-doped ZnO nanoparticles combines the benefits of both green chemistry and the enhanced properties of the doped nanoparticles, making it a promising approach for sustainable wastewater treatment.

2.7 Applications of Fe-doped ZnO Nanoparticles in Dye Removal

Fe-doped ZnO nanoparticles have shown great promise to remove various dyes from waste water, including methylene blue. Their enhanced adsorption capacity, Stability and photocatalytic activity under visible light make them ideal candidates to purify water contaminated with dye. Several studies have demonstrated Effect of iron-doped ZnO on methylene blue removal with the nanoparticles achieving high removal efficiencies under various experimental conditions (Bhattacharyya et al., 2015; Zhang et al., 2018). These studies suggest that Fe-doped ZnO

nanoparticles not only improve methylene blue removal efficiency but also offer advantages in terms of reusability and stability, making them more practical for real-world applications.

2.8 Adsorption Mechanism of Methylene Blue on the Surface of Fe-Doped ZnO Nanoparticles

The adsorption mechanism of methylene blue (MB) on the surface of Fe-doped ZnO nanoparticles is a complex process that involving several key interactions between the dye molecules and the surface of the nanoparticles. These interactions are influenced by the properties of both the dye (MB) and the Fe-doped ZnO material, as well as external conditions such as pH, temperature, and the concentration of the dye. Below is an expanded explanation of the adsorption mechanism.

2.8.1 Surface Characteristics of Fe-Doped ZnO Nanoparticles

Fe-doped nanoparticles are characterized by increased surface area, high porosity, and the presence of surface functional groups. The doping of Fe into ZnO modifies its electronic structure and surface properties. The Fe ions can introduce surface charge imbalances, modify the electronic distribution, and create new active sites on the surface. These features play an important role in the adsorption of methylene blue molecules. **Surface Charge:** The presence of Fe ions on the ZnO surface changes the surface charge, which may affect the electrostatic interaction between the nanoparticles and MB dye. Fe-doped ZnO is generally more negatively charged under basic conditions, which could lead to stronger electrostatic attraction between the positively charged MB molecules and the negatively charged surface. **Surface Defects and Active Sites:** Fe doping may also create vacancies and defects in the ZnO structure, providing additional active sites for adsorption. These sites can interact with the MB dye through various mechanisms such as hydrogen bonding and van der Waals forces, or even chemisorptions

2.8.2. Electrostatic Interactions

Methylene blue is a cationic dye, Methylene blue is a cationic dye, meaning it has a positive charge in aqueous solution. Especially at neutral or basic pH. Electrostatic interactions between the negatively charged nanoparticle surface and positively charged MB molecules are the main driving force for the adsorption process. This interaction allows MB molecules to adsorb on to the surface

through an ion-exchange process. **Attraction to the Surface:** In environments where the pH favors a negative charge on the nanoparticle surface (e.g. $\text{pH} > 7$). The electrostatic attraction between positively charged MB ions and the iron doped ZnO surface is maximum. The positively charged MB molecules are drawn toward the nanoparticle surface, leading to adsorption. **pH Dependence:** The efficiency of adsorption is highly pH-dependent. At lower pH values the surface Fe-doped ZnO nanoparticles tends to become positively charged, reducing electrostatic attraction with the MB dye thus decreasing the adsorption capacity. On the other hand, the higher the pH, values, the surface becomes more negatively charged, enhancing the adsorption of MB.

2.8.3 Surface Complexation and Hydrogen Bonding

In addition to electro static forces, surface complexation can occur between the dye molecules and the surface of Fe-doped ZnO. This interaction involves the formation of chemical bonds between functional groups on the nanoparticle surface (such as hydroxyl groups, oxygen vacancies, or metal cations) and the MB dye. **Hydroxyl Groups:** The surface of ZnO typically contains hydroxyl groups (-OH) due to its interaction with water. These groups can participate in hydrogen bonding with the MB dye molecules, further stabilizing the adsorption of MB on the nanoparticle surface.

Fe(III) Coordination: Iron ions (Fe^{3+}) introduced into ZnO may also coordinate with the functional groups of MB, enhancing the binding between the dye and the a nanoparticle surface. Fe ions on the surface can form coordination bonds with the nitrogen atoms in the MB structure.

2.8.4 Photocatalytic Effect (If Applicable)

In some cases, Fe-doped ZnO nanoparticles can act as photo catalysts. Upon exposure to light, these nanoparticles can generate electron-hole pairs that may interact with the methylene blue dye in a photo degradation process. This can occur through the generation of reactive oxygen species (ROS), such as hydroxyl radicals ($\bullet\text{OH}$) or superoxide ions ($\text{O}_2^{\bullet-}$), which can degrade the dye molecules. This mechanism, while not directly related to adsorption, can influence the overall behavior of MB in the presence of Fe-doped ZnO nanoparticles.

2.8.5 Adsorption Isotherms

Fe-doped ZnO nanoparticles are often valued for their reusability in adsorption processes. After the adsorption of MB, the nanoparticles can potentially be regenerated and reused through washing or by altering the pH or temperature to release the dye from the surface. The stability and regeneration

of the nanoparticles are critical for their application in industrial processes, and they are often evaluated in terms of their adsorption capacity over multiple cycles. The adsorption of methylene blue on the surface of Fe-doped ZnO nanoparticles is governed by a combination of electrostatic forces, surface complexation, and, in some cases, photocatalytic effects. The surface properties of the nanoparticles, such as charge distribution, the presence of hydroxyl groups, and iron doping, play significant roles in determining the efficiency and mechanism of adsorption. Understanding these interactions is crucial for optimizing the use of Fe-doped ZnO nanoparticles in environmental and industrial applications, particularly for dye removal and water treatment processes

2.8.6 Kinetics of Adsorption

The adsorption of MB on iron-doped ZnO nanoparticles can be evaluated by studying the kinetics of the process. Common models for kinetic analysis include the pseudo-first-order model and the pseudo-second-order model. The adsorption rate can depend on the concentration of MB. The accessibility of surface sites and the temperature .Pseudo-first-order kinetics: This model assumes that the adsorption rate is proportional to the MB concentration on the nanoparticle surface. Pseudo-second-order kinetics: This model implies that the adsorption rate depends on the square of the MB concentration, indicating that the adsorption may involve the formation of chemical bonds or more complex interactions.

2.8.7 Regeneration and Reusability

Iron-doped ZnO nanoparticles are often valued for their reusability in adsorption processes. Once adsorbed onto MB, the nanoparticles can be potentially regenerated and reused by washing them or by changing the pH or temperature to release the dye from the surface. The stability and reusability of the nanoparticles are of great importance for their application in industrial processes and are often evaluated in terms of their adsorption capacity over multiple cycles. The adsorption of methylene blue on the surface of iron-doped ZnO nanoparticles is controlled by a combination of electrostatic forces, surface complexation, and in some cases, photocatalytic-effects

The surface properties of the nanoparticles, such as charge distribution, presence of hydroxyl groups, and iron doping, play a significant role in determining the adsorption efficiency and mechanism. Understanding these interactions is important for optimizing the use of iron-doped ZnO nanoparticles in environmental and industrial applications, particularly in dye removal and water purification processes.

2.9 Knowledge Gaps and Research Opportunities

Despite the promising potential of Fe-doped ZnO nanoparticles synthesized using green methods, several knowledge gaps remain. First, while many studies have explored the synthesis and characterization of Fe-doped ZnO, few have focused on the use of plant extracts, particularly *Justicia adhatoda*, for nanoparticle synthesis. Additionally, there is a need for more comprehensive studies on the optimization of synthesis conditions to maximize the efficiency of Fe-doped ZnO nanoparticles in dye removal. Finally, while the adsorption and photocatalytic properties of Fe-doped ZnO nanoparticles have been well-documented, their practical application in real-world wastewater treatment scenarios, including large-scale pilot studies and assessments of their long-term stability and reusability, remains underexplored.

CHAPTER THREE

3 MATERIAL AND METHODS

3.1 Apparatus and Instruments

The major apparatus and instrument used during this thesis study were analytical balance, mortar, and pestle, grinding machine 250 ml plastic bottles, Sieves(200-250 mm size),pH meter,50-250 ml size beaker, measuring cylinder, conical flask, digital oven, UV-DRS(UV-Vis NIR CLB, Model V-770), ATR-FTIR(Perkin Elmer spectrum 65model FTIR), P-XRD (XRD-7000, SHIMADZU Corporation, Japan),crucible, volumetric flasks(50-250ml),test tubes, and Whatman filter paper, etc

3.2 Chemical and reagents

Most of the chemicals used in this thesis study were analytical grades obtained from different chemical suppliers. The *Justicia adhatoda* leaf was collected from Wolkite town local area. The chemicals used include analytical grade of iron (III) chloride hexa-hydrate, zinc acetate, oxalic acid, methylene blue, and distilled water.

3.3 Experimental site

The synthesis of iron-doped and undoped zinc oxide adsorbent and all batch adsorption experiments were carried out at the Department of Applied Chemistry Laboratory of Wolkite University. The synthesized samples were characterized at Addis Ababa science and Technology University.

3.4 Methods and Procedures

3.4.1 Collection of *Justicia Adhatoda* Plant Leaf

Justicia adhatoda leaves were collected from the local area of Wolkite town, Guraghe Zone, Ethiopia. To remove unwanted material, leaf samples were washed repeatedly with tap water and then with distilled water. To eliminate any remaining moisture, the cleaned *Justicia adhatoda*

the leaves were completely dried at room temperature, open, and in the shade for approximately seven days. Using an electric grinding machine, the dried leaves were ground into a fine powder. The material was then dried, ground, and stored in preparation for further processing[50].

3.4.2 Preparation of *Justicia adhatoda* Leaf Extract

The crushed *Justicia adhatoda* leaf powder (30 g) was boiled in 200 ml of double distilled water for 15minutes. The resulting aqueous leaf extract was cooled and filtered through Whatman No. 1 filter paper. The prepared leaf extract was stored in sterile containers at 4°C for future use. [51].

3.4.3 Preparation of Undoped zinc oxide

A 0.2M zinc precursor solution was prepared by dissolving 8.477g of zinc acetate in 100 ml of distilled water [52]. In another flask, 20 ml of the aqueous extract of the plant was taken and placed on a magnetic stirrer. Then, the zinc acetate solution was mixed with the extract by continuous stirring (200 rpm) at 60 °C for 3 h to form a gel. The resulting mixture was continuously stirred for 10min. 2M sodium hydroxide solution was added drop wise to the mixture until the pH reached 12. The solution was stirred for an additional 3 h to evaporate the solvent and cool the gel mixture to room temperature. The gel was then transferred to a Petri dish and dried in a convection oven at 60 °C for 24 h. Once dried, the sediment was ground using a mortar and pestle. The dried and crushed sediment was calcined in an oven at 750°C for 3 h to obtain nanoparticles [53].

3.4.4 Preparation of Fe-doped ZnO nanoparticles

First, 8.477 g of zinc acetate was mixed with 100 ml of deionized (DI) water. A required amount of iron chloride was then added to the zinc acetate solution to achieve 5% and 10% molar doping of Fe. Plant extract (50 ml) was added to the solution with continuous stirring (200 rpm) for 3 hours at 60°C to facilitate gel formation. The resulting mixture was stirred continuously for more than 10 minutes. Then, 2 M sodium hydroxide solution was added drop wise to the mixture until the pH reached 12. After 30 minutes, the nanoparticles (NPs) were obtained after centrifugation (1000 rpm for 15 min), the nanoparticles were washed several times with ethanol and deionized water, and then dried in an oven at 100 °C. Finally, the dried nanoparticles were calcined in a muffle furnace at 400 °C for 3 h. The calcined nanoparticles were used for further studies [52, 53].

3.5 Characterization studies

The synthesized Fe-doped and undoped zinc oxide nanoparticles were characterized using various instrumental techniques to confirm the success of the synthesis procedure and to determine key properties such as particle size, functional groups, and other characteristics required for the material to be used as an adsorbent. In this regard, UV-DRS (UV-Vis NIR CLB, Model V-770), ATR-FTIR (Perkin Elmer Spectrum 65 FTIR), and P-XRD (XRD-7000, SHIMADZU Corporation, Japan) were employed to characterize the synthesized samples.

3.6 Removal of Methylene blue using Fe-doped zinc oxide nanoparticle by sorption

3.6.1 Preparation of working standard solutions

In the sorption studies, methylene blue (MB) powder was used as the adsorbate in this work. To prepare the MB stock solution, 1 g of MB was dissolved in 1000 mL of distilled water to obtain 1000 mg/L. Additional working standard solutions of MB at concentrations of 5, 10, 15, and 20 mg/L were prepared from the 1000 mg/L standard dye solution using the dilution rule [54].

3.6.2 Batch sorption experiment

The removal of an aqueous solution containing varying concentrations of methylene blue (MB) was used to assess the batch-mode sorption capabilities of the synthesized samples [54]. Sorption studies were conducted in a 200 mL conical flask, where various parameters were examined. By changing one parameter while keeping the others constant, the influence of parameters such as pH, adsorbent dosage, dye concentration and contact time can be evaluated. This approach allows for the examination of adsorption kinetics and the determination of how these factors influence the removal capacity. After each sorption experiment, samples were withdrawn from the flask and filtered using Whatman filter paper. Range of experimental variables explored included pH values (3, 5, 7, and 9), adsorbent dosages (0.02, 0.05, 0.08, and 0.12 g), initial dye concentrations (5, 10, 15, and 20 mg/L) and contact times (25, 45, 65 and 85 min). The absorbance of the filtrate was measured using a UV-visible spectrophotometer set to a maximum wavelength of 664 nm. Equation 1 can be used to evaluate the removal efficiency of iron-doped zinc oxide nanoparticle complexes [54].

$$\text{Removal efficiency (\%)} = \frac{A_i - A_t}{A_i} \times 100 \dots\dots\dots \text{Eq(1)}$$

Where, A_i is the initial absorbance of dye solution, and A_t is the dye solution absorbance at a certain reaction or degradation time

3.6.3 Sorption kinetic studies

The most popular models for fitting the kinetic research experiment to examine the sorption rate processes are pseudo-1st and pseudo-2nd models. The residence duration of the adsorption reaction is determined by the solute uptake rate, which is described by the sorption kinetics [55].

Pseudo-first order kinetics determined using the following equation (2)

$$\ln(q_e - q_t) = \ln q_e - K_1 * t \dots \dots \dots (Eq2)$$

The pseudo-second-order dynamics are determined by the following equation (3)

$$\frac{t}{q_t} = \frac{1}{K_2 q_e^2} + \frac{1}{q_e} * t \dots \dots \dots (Eq3)$$

3.6.4 Reusability test of Fe-doped zinc oxide nanoparticles

After adding the optimal sorbent dosage of Fe-doped ZnO nanoparticles to 50 ml of MB solution at the desired concentration, the mixture was agitated for the optimal duration. Following centrifugation, the dye-adsorbed nanoparticles were separated, and desorption was carried out by adding distilled water. For the second adsorption cycle, the desorbed sorbent nanoparticles were isolated and re used. To evaluate the methylene blue dye removal efficiency, the same process was repeated at least five times[55].

CHAPTER FOUR

4.RESULT AND DISCUSSION

4.1 Characterization of synthesized adsorbent

4.1.1 UV-Vis DRS Analysis of ZnO and Fe-ZnO NPs

Figure 4 shows the UV-visible spectra of the as-synthesized zinc oxide (ZnO) and alloyed Fe-ZnO samples at room temperature. The spectra clearly show that both ZnO and Fe-ZnO exhibit absorption peaks and that ZnO absorbs at around 330 nm whereas Fe-ZnO absorbs at around 340nm. This shift in the absorption peak is an important observation since it shows a red shift (or shift towards larger wavelengths)

In the alloyed Fe sample compared to the unalloyed ZnO. This shift in the absorption spectrum is generally associated with the introduction of Fe into the ZnO lattice. The red shift observed in the UV-visible ZnO spectrum alloyed with iron can be explained by the interaction between the ZnO sp electrons and the localized d electrons of the Fe (iii) ions. These interactions alter the electronic structure of ZnO, thereby changing its optical properties. In particular, the inclusion of Fe ions in the ZnO lattice creates new energy states in the domain structure, which absorb light at a higher wavelength than pure ZnO. This phenomenon is also observed as a change in the shade of the material appearance, while in alloyed Fe ZnO, the color changes from white (illegal ZnO) to a reddish-yellow hue, further confirming the electronic changes upon focusing of Fe. The observed red shift and shade change in alloyed Fe- ZnO are consistent with previous studies reporting spectral shifts for alloyed Fe ZnO samples. These results indicate that Fe doping in the ZnO matrix alters the electronic structure of the material, thereby affecting its optical absorption properties. This is consistent with the general understanding of alloy-induced semiconductor changes, where the inclusion of metal ions can lead to changes in optical absorption, which has also been observed in synthetic samples [56].

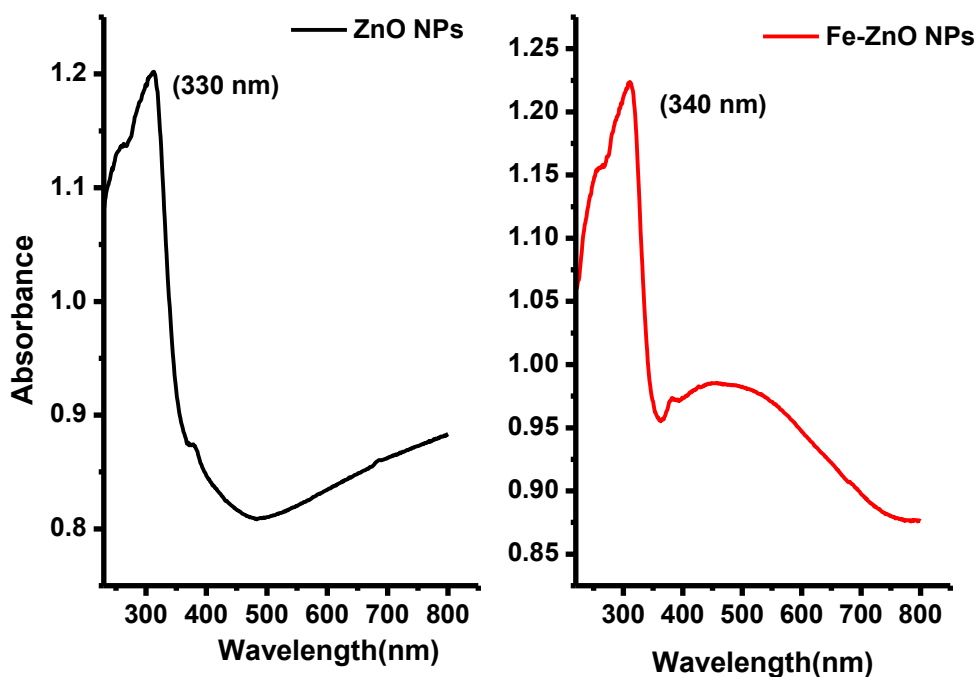


Figure 4: UV-DRS spectrum of ZnO and Fe-ZnO NPs

4.1.2 XRD analysis of ZnO and Fe-ZnO NPs

Figure 5 shows the X-ray diffraction (XRD) patterns of pure ZnO and Fe-doped ZnO nanoparticles (NPs). The diffraction pattern of pure ZnO follows the standard reference card (JCPDS card no. 01-074-0534) indicating the hexagonal crystal structure of wurtzite. This hexagonal structure is clearly observed in the XRD pattern, with characteristic peaks at 31.70° , 34.42° , 36.12° , 47.50° , 56.58° , 62.80° , 66.62° , and 67.82° . The peaks correspond to the (100), (002), (101), (102), (110), (103), (112), and (201) diffraction planes, respectively, which are consistent with the typical XRD pattern of ZnO nanoparticles. When doped with iron (Fe), the ZnO nanoparticles retain the hexagonal wurtzite structure, as evidenced by the presence of the same diffraction peaks in the XRD pattern. The Fe-doped ZnO nanoparticles exhibit similar 2θ values to pure ZnO, indicating that Fe doping does not significantly change the ZnO crystal structure. However, a notable change in the XRD pattern is a slight broadening of the base peak in the Fe-doped ZnO sample compared to the undoped ZnO. This broadening can be explained by the incorporation of Fe ions into the ZnO lattice, which may induce distortions or defects that affect the crystallinity of the material. The crystallite sizes of undoped and Fe-doped ZnO nanoparticles were calculated using the Debye-Scherrer equation (Eq. 4) based on X-ray diffraction data. The broadening of the peaks for the Fe-

doped ZnO sample indicates a decrease in the crystallite size, which is typical when foreign ions such as Fe are introduced into the ZnO lattice. The Debye–Scherrer equation provides a method to estimate the average crystallite size from the full width at half maximum (FWHM) of the diffraction peaks, allowing a quantitative comparison between the two samples [48].

$$D = \frac{k\lambda}{\beta \cos\theta} \dots\dots\dots(Eq4)$$

The crystalline size (D) of the particles are estimated where the wavelength λ for X-ray is 0.154 nm, the shape factor k has a value of 0.89 if the shape is unknown, the average diameter of the crystal D in Å, α is the Bragg’s angle in degree and β is the half-height of angle in radian.

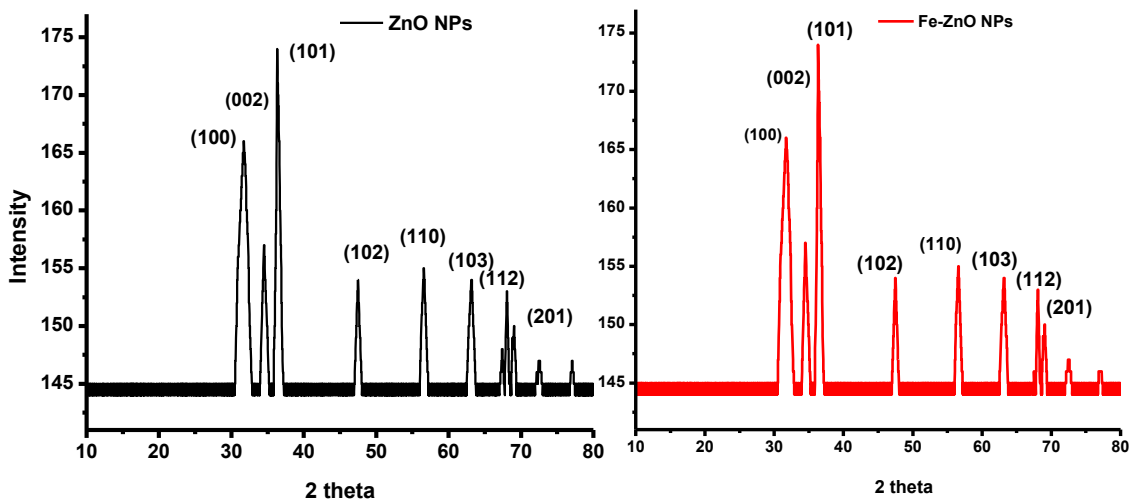


Figure5:XRD spectrum of ZnO and Fe doped ZnO NPs

The average particle sizes of the synthesized ZnO nanoparticles and Fe-doped ZnO were 24 nm and 20 nm, respectively. The decrease in particle size with Fe doping is consistent with similar studies. For example, Robina Ashrafetal [57] synthesized undoped ZnO and Fe-doped ZnO nanoparticles and reported that the particle size decreased from 29 nm for undoped ZnO to 19 nm for Fe-doped ZnO with increasing Fe content. This size decrease may be due to the following reasons: The inclusion of Fe ions in the ZnO lattice causes stress and defects, which makes the crystal structure

finer. Similarly, Hamid et al. [58] and FalakNaz et al. [59] synthesized both undoped and chromium-doped ZnO nanoparticles and observed similar trends. In their study, the particle size of nanoparticles determined by X-ray diffraction decreased from 30.07 nm for undoped ZnO to 28.14 nm for chromium-doped ZnO with chromium doping. These results support the idea that doping with metal ions such as Fe and Cr can affect the ZnO crystal size, and that the particle size decreases due to the inclusion of dopant impurities, which usually destroy the crystal lattice and affect the growth process.

4.1.3 FTIR Analysis of ZnO, Fe-ZnO and Plant extract

Figure 6 shows the FTIR spectra of undoped ZnO, Fe-doped ZnO nanoparticles, and *Justicia adhatod* leaf extract. FTIR spectroscopy provides valuable information about the functional groups, molecular structure, and intermolecular interactions of the samples, and therefore, it was used to study the vibrational bands of calcined ZnO and Fe-doped ZnO nanoparticles at room temperature. The FTIR spectra of Fe-doped ZnO and ZnO nanoparticles show an intense peak at 3340 cm^{-2} , which corresponds to the stretching vibration of the O-H bond of the solvent (probably due to adsorbed water or hydroxyl groups). The peak at 2850 cm^{-2} is attributed to the stretching vibration of the C-H bond of CH_2 and CH_3 groups, which are typical of organic compounds. The faint band around 2340 cm^{-2} represents the absorption from the ambient CO_2 , which interacts with the metal cations of the sample. Further analysis revealed the presence of carbonyl (C=O) stretching at 1632 and O-H bending absorption at 1410 cm^{-2} , both of which are associated with the alcohol functional group. The C-O stretching mode of secondary alcohols is responsible for the peak at around 1085 cm^{-2} [60]. The peak observed in the range of 1700–1000 cm^{-1} . Also, the peak at 460 cm^{-2} corresponds to the FeO stretching vibration commonly observed in Fe-doped materials. The lower bonding frequency of FeO compared to ZnO is due to the relatively lower mass of Fe atoms compared to ZnO. Zn confirms that Fe is incorporated into the ZnO lattice. This indicates that Fe has been successfully doped into the ZnO crystal structure. The FTIR spectrum of the *Justicia Adhatoda* leaf extract shows several peaks that provide additional insight into the organic components of the plant material. The broad peak at 3352 cm^{-2} is attributed to the OH stretching vibration of alcohol or phenol groups, while the peak at 2918 cm^{-2} corresponds to the CH stretching vibration of alkanes. The peak at 2440 cm^{-2} confirms the presence of the typical $\text{C}\equiv\text{C}$ stretching vibration of alkynes. Additionally, the peak at 1648 cm^{-2} is associated with the stretching vibration of the

aldehyde carbonyl (C=O) group [61]. This functional group likely plays a role in blocking or stabilizing the nanoparticles during synthesis.

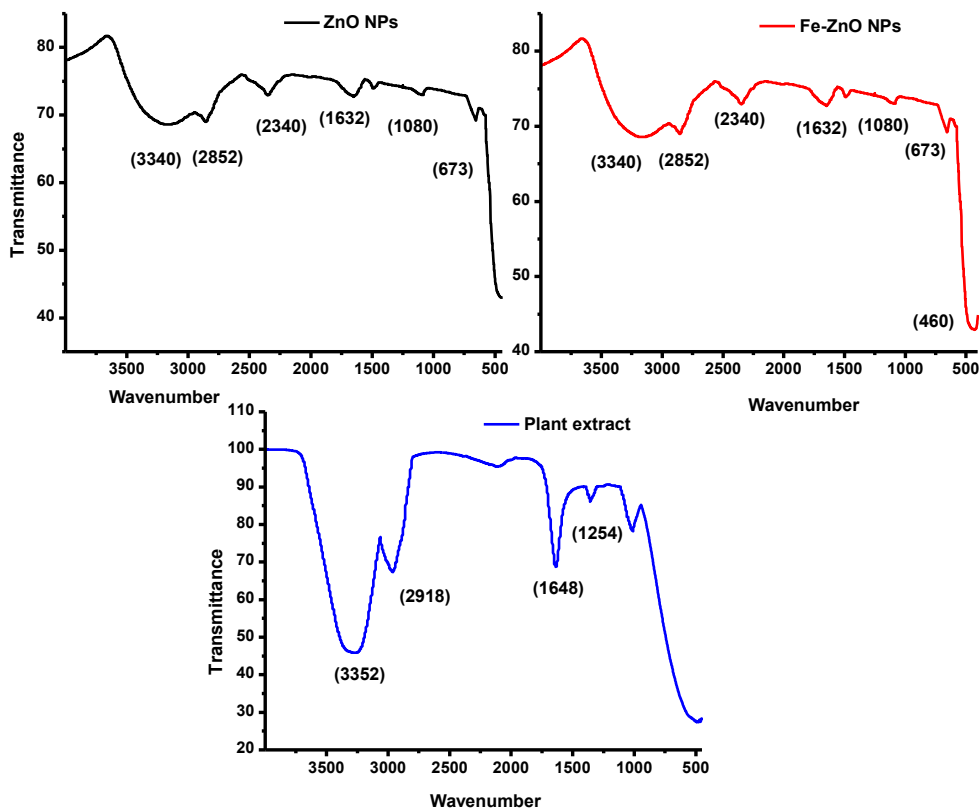


Figure 6: FTIR spectra of ZnO, Fe doped ZnO and Plant extract

4.2 Optimization of adsorbent for removal of MB dye from aqueous solution

4.2.1 Calibration plot of working methylene blue standard solution

The residual concentration of methylene blue (MB) dye in the filtrate after adsorption in aqueous solution using synthesized ZnO nanoparticles (NPs) and iron-doped ZnO as adsorbents, was determined through a calibration plot. The graph was generated by measuring the absorbance of MB dye solution at 664 nm, which is the maximum absorption wave length for methylene blue.

The absorbance values for different known concentrations of MB were recorded to establish the calibration curve.

Table 2 presents the data for the MB dye standard solutions, and Figure 7 illustrates the resulting calibration plot. This plot enables the determination of the dye concentration in unknown samples by correlating their absorbance to the known concentrations of the standard solutions.

Table 2: Methylene blue dye working standard solution calibration data

The initial concentration of MB(mg/L)	Absorbance
5	0.015
10	0.029
15	0.041
20	0.053

From Table 2, we can conclude that there is a linear relationship between the concentration of methylene blue dye and its absorbance at 664 nm within the tested concentration range (5–20 mg/L). This allows for the accurate determination of MB concentrations in experimental samples, particularly for assessing the effectiveness of the ZnO and Fe-doped ZnO nanoparticles as adsorbents in the removal of MB dye from aqueous solutions

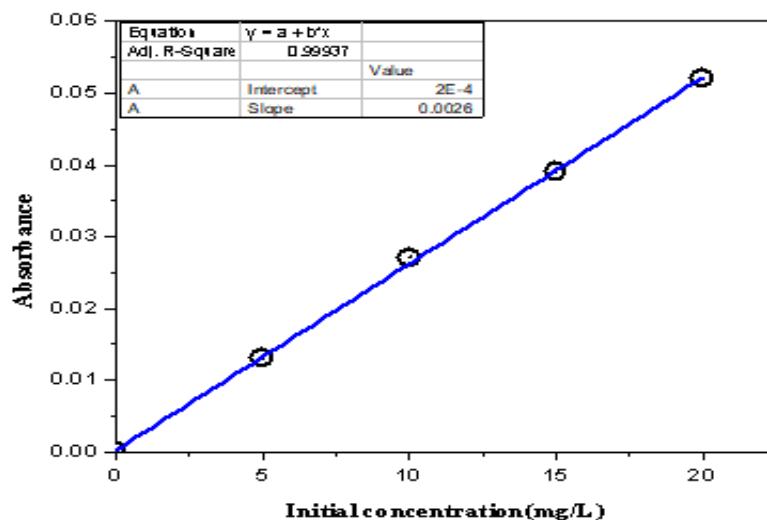


Figure 7: Calibration plot of working MB standards solution.

4.3 MB dye adsorption by using ZnO and Fe doped ZnO NPs

4.3.1 Effect of pH on the Adsorption of Methylene Blue Dye

The pH of the dye solution plays an important role in the adsorption process and has a great influence on the adsorption capacity of the adsorbent material. This is mainly due to the effect of pH on the surface charge of the adsorbent, the degree of ionization of the dye molecules, and the interaction between the functional groups. These factors determine how well the adsorbent interacts with the dye molecules and can adsorb the dye molecules from the solution. For methylene blue (MB), a cationic dye, the pH of the solution directly affects the charge distribution on both the dye and the adsorbent surface. ZnO and Fe-doped ZnO nanoparticles (NPs), which are commonly used as adsorbents, show changes in surface charge depending on the solution pH. This ultimately affects the electrostatic interaction between the adsorbent and the dye molecules, which is the key to the adsorption process. At low pH values, the surfaces of ZnO and Fe-ZnO nanoparticles tend to be positively charged due to the protonation of the surface hydroxyl groups (Zn-OH^+) of the adsorbent. In this scenario, the positive charge of the adsorbent competes for binding sites with the cationic dye molecules, resulting in a decrease in the adsorption capacity at pH values below the point of zero charge (pHpzc). The pH pzc is the pH at which there is no net charge on the adsorbent surface. Below this pH, the surface is predominantly positively charged, whereas above pHpzc, it is negatively charged. For cationic dyes such as positively charged MB, the adsorption capacity decreases at pH values below pHpzc due to the repulsion between the positively charged surface and the dye molecules. As the pH increases above pHpzc, the surfaces of ZnO and Fe-ZnO nanoparticles become negatively charged, resulting in stronger electrostatic attraction between the negatively charged surface and the positively charged dye molecules. Therefore, the adsorption of MB dye significantly increases as the pH of the solution moves above pHpzc, and stronger adsorption occurs at pHpzc due to enhanced electrostatic interactions.

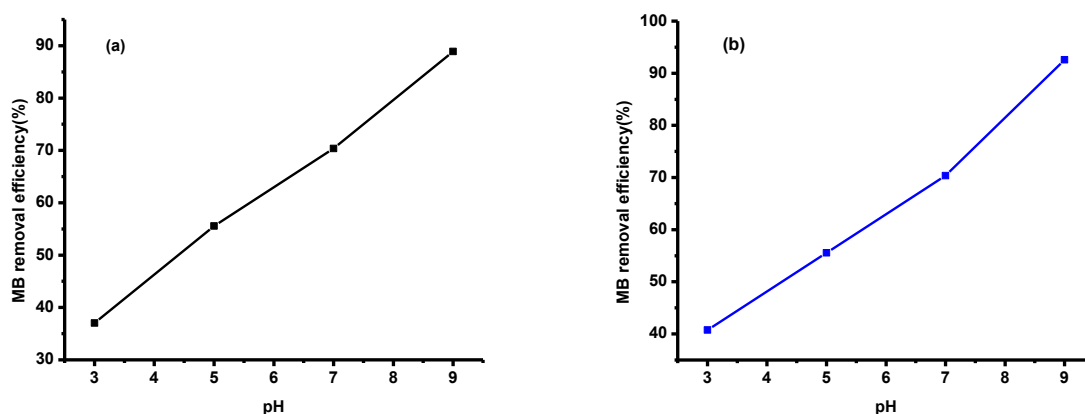


Figure 8: Effect of pH on MB dye removal by (a) ZnO NPs, & (b) Fe-ZnO NPs

Investigation of the effect of pH on dye adsorption, an experimental study was conducted by adding 40 mg of ZnO and Fe-doped ZnO nanoparticles to a solution containing 10 mg/L of methylene blue (MB). The pH of the solution was varied between 3 and 9, and the system was allowed to equilibrate for a contact time of 45 minutes.

The results, shown in Figure 8(a & b), illustrate a clear trend: dye uptake increased as the pH of the solution increased. At lower pH values (pH 3), the adsorption of MB was relatively low. This can be attributed to the protonation of surface groups on the nanoparticles, which results in the surface being more positively charged, thus repelling the positively charged MB dye molecules.

When the pH increased to pH 9, the adsorption capacities of ZnO and Fe-doped ZnO nanoparticles increased significantly. This is consistent with the shift of the surface charge of the adsorbent from positive to negative when the pH exceeds pH_{pzc} , which promotes stronger electrostatic interactions with the cationic MB dye. The removal efficiency of MB increased significantly when the pH changed from acidic (pH 3) to alkaline (pH 9). ZnO nanoparticles showed a significant increase in adsorption, with the removal efficiency increasing from 37.03% at pH 3 to 88.88% at pH 9. Fe-ZnO nanoparticles showed an even more significant improvement, with the removal efficiency increasing from 40.74% at pH 3 to 92.59% at pH 9. The significant increase in adsorption at higher pH values highlights the effectiveness of the nanoparticles. In MB dye adsorption on Fe-doped ZnO appears to occur due to increased electrostatic attraction at alkaline pH, where both the adsorbent surface and the dye molecules are more favorably charged for adsorption.

4.3.2 Effect of Adsorbent Dosage on the Adsorption of Methylene Blue Dye

Adsorbent dosage is an important factor that greatly affects the adsorption capacity of nanoparticles including ZnO and iron-doped ZnO (Fe-ZnO) for the removal of pollutants such as methylene blue (MB) dye from aqueous solution. In this experiment, the effect of varying the adsorbent dosage on

the MB removal efficiency was investigated at pH 9. At pH 9, the adsorption process was expected to be more efficient due to the negative surface charge of the adsorbent, which promotes the electrostatic attraction of the cationic dye.

The experiment was conducted at a fixed initial concentration of 10 mg/L of MB dye, and the adsorbent dosage was varied from 20mg to 120mg for both ZnO and Fe-ZnO nanoparticles. The contact time was kept constant at 45minutes to ensure that the adsorption equilibrium was reached

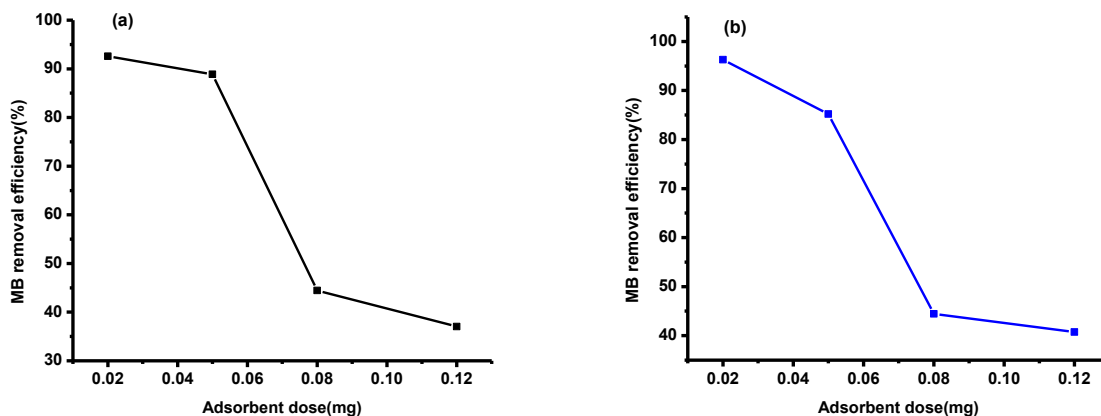


Figure 9: Effect of adsorbent dose on MB dye removal by (a) ZnO NPs, & (b) Fe-ZnO NPs

Results and Discussion

The findings, shown in Figure9, reveal that the removal efficiency of MB dye increased with the increase in adsorbent dosage initially, but after a certain point, further increases in the adsorbent do seled to a decline in dye removal efficiency. Specifically, at an adsorbent dosage of 20mg, the Removal efficiency was at its highest for both ZnO and Fe-ZnO nanoparticles, with ZnO adsorbing 92.59% of the MB dye and Fe-ZnO adsorbing 96.29% of the dye. As the adsorbent dosage was increased beyond 20 mg, the removal efficiency started to decrease. For ZnO nanoparticles, the removal efficiency dropped from 92.59% at 20 mg to 37% at 120 mg. For Fe-ZnO nanoparticles, the removal efficiency dropped from 96.29% at 20 mg to 40.74% at 120 mg.

As the adsorbent dosage increases from 20 mg, the number of available adsorption sites also increases, leading to higher removal efficiency. The increased surface area of the nanoparticles provides more sites for the cationic MB dye to bind via electrostatic attraction. When the dosage was increased beyond 20mg, the dye removal efficiency decreased. This is due to the fact that the adsorption sites become more dispersed as more nanoparticles are added, resulting in less effective interaction between the dye molecules and the adsorbent surface. Additionally, at higher dosages, there may not be enough MB dye molecules present in the solution to interact with all the available adsorption sites, leading to unsaturated adsorption. This results in wasted adsorption sites on the nanoparticles that cannot effectively bind more dye molecules, thereby lowering the overall adsorption efficiency.

At high dosages (e.g., 120 mg), the adsorbent surfaces become saturated, and any additional increase in the dosage does not lead to further significant removal of MB dye. The excess nanoparticles may also form aggregates or become less efficient in the adsorption process due to the limited number of dye molecules available to occupy the adsorption sites.

Based on the results of the experiment, it was concluded that the optimal adsorbent dosage for both ZnO and Fe-ZnO nanoparticles in the removal of methylene blue (MB) from aqueous solutions was 20 mg. At this dosage, the adsorption capacity was maximized, and the removal efficiency was highest. As the adsorbent dosage increased beyond 20mg, the adsorption efficiency began to decline due to factors such as saturation of adsorption sites and insufficient dye molecules to interact with the additional adsorbent material. Therefore, the 20 mg dosage was selected as the optimal amount of nanoparticle adsorbent for further experimental investigations. This finding underscores the importance of selecting the correct adsorbent dosage to balance between having sufficient adsorption sites for the dye molecules and avoiding unnecessary excess material that does not contribute to the adsorption process.

4.3.3 Effect of Contact Time on the Adsorption of Methylene Blue Dye

Equilibrium time is an important parameter in the design of an efficient and economical wastewater treatment system. It represents the time required for the system to reach a state where the dye adsorption rate and desorption rate are equal and there is no significant change in the dye molecule concentration in the solution. This time is important for determining the effectiveness of the adsorbent in removing pollutants and for optimizing the operating parameters in practical

applications. In this study, the adsorption of methylene blue (MB) dye was investigated using 20 mg ZnO and Fe-ZnO NPs as adsorbents at a fixed dye concentration of 10 mg/L and pH 9. The effect of contact time on MB adsorption was evaluated over a range of durations from 25 to 85 min. Figure 10 shows the adsorption kinetics of ZnO and Fe-ZnO nanoparticles and how the percentage of removed dye changes with time. The results show that the adsorption process follows a two-step trend, i.e., the adsorption of MB dye increases rapidly during the first 25 min of contact time. For ZnO nanoparticles, the dye removal rate increases from 59.20% to 92.59%, while for Fe-ZnO nanoparticles, the removal rate increases from 40.74% to 96.29%.

This high initial adsorption rate may be due to the large number of accessible and active adsorption sites on the nanoparticle surface. In the early stage of the reaction, many sites on the surface are empty, allowing dye molecules to easily interact with the adsorbent. The concentration gradient between the dye in solution and the adsorbent surface is steep, which promotes rapid penetration of dye molecules into the adsorbent surface. Slower adsorption and approach to Equilibrium (After 25 Minutes):

After the initial phase, the adsorption rate starts to slow down as the available adsorption sites become increasingly occupied. This results in a gradual decrease in the rate of adsorption as the concentration gradient diminishes. At this point, the system is approaching equilibrium, where the rate of dye molecules adsorbing to the surface of the nanoparticles is approximately equal to the rate at which dye molecules are desorbing from the surface. The adsorption efficiency begins to stabilize, with the removal percentage reaching a near-constant value. For both ZnO and Fe-ZnO NPs, the dye removal rate levels off after approximately 45 minutes, indicating that equilibrium has been achieved. The adsorption capacity of the

Nanoparticles is largely saturated, and additional contact time does not lead to as significant increase in dye removal.

The rapid adsorption observed at the beginning can be explained in terms of:

Large number of available sites: At the start of the reaction, the adsorbent surface is largely unoccupied, providing sample vacant sites for the dye molecules to adsorb.

High concentration gradient: The difference between the dye concentration in solution and on the adsorbent surface is high at the beginning, which drives the adsorption process.

As the reaction proceeds, the concentration gradient decreases, and the available adsorption sites on the ZnO and Fe-ZnO nanoparticles become saturated. Once a significant portion of the surface sites are occupied by the dye molecules, the adsorption rate slows down, leading to the system approaching adsorption equilibrium. This is a common feature in adsorption processes, where the adsorption capacity increases rapidly at first and then levels off as equilibrium is reached.

The experiment demonstrated that equilibrium in the adsorption of methylene blue dye using ZnO and Fe-ZnO nanoparticles is reached after approximately 45 minutes of contact time. The first 25 minutes show a sharp increase in dye removal, attributed to the availability of free adsorption sites and a high concentration gradient. After 45 minutes, the removal efficiency stabilizes as the adsorbent surfaces become saturated. ZnO NPs achieved a removal efficiency of 92.59% after 45 minutes, while Fe-ZnO NPs reached 96.29% removal. These results suggest that both materials are highly effective for MB dye removal, with Fe-doping further improving the adsorption capacity. The contact time of 45 minutes was found to be optimal for achieving maximum dye removal, beyond which increasing the contact time did not significantly affect the removal efficiency. This information is valuable for the design of efficient wastewater treatment systems, as it provides insights into the necessary contact time for optimal dye removal. Equilibrium time can thus be used to optimize system designs and reduce the costs associated with prolonged treatment times

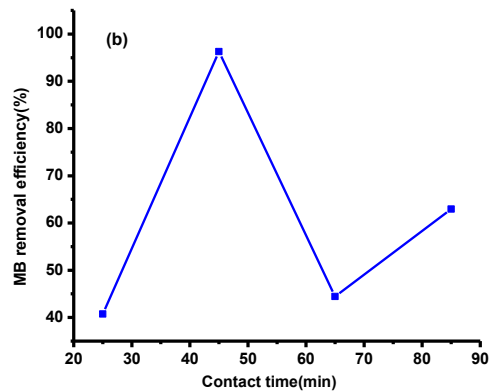
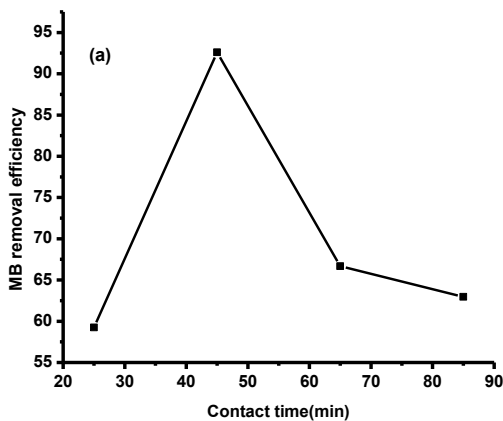


Figure 10: Effect of contact time on MB dye removal by (a) ZnO NPs, & (b) Fe-ZnO NPs

4.3.4 Effect of initial concentration

A series of experiments were conducted to investigate the impact of initial methylene blue (MB) dye concentration on the adsorption efficiency of ZnO and Fe-ZnO NPs. In these tests, varying concentrations of MB solution (5, 10, 15, and 20 mg/L) were used with a fixed adsorbent dosage of 20mg of ZnO and Fe-ZnO NPs at pH 9 for a contact time of 45minutes. The results, presented in Figure 11, show a clear trend in the adsorption behavior with respect to changing dye concentrations. At lower starting concentrations of MB (5mg/L), the adsorption process is highly efficient, with ZnO NPs and Fe-ZnO NPs adsorbing around 95.23% and 99.52% of the dye, respectively. This indicates that at lower dye concentrations, there is a higher availability of active sites on the adsorbent surface for the dye molecules to bind, resulting in a greater removal efficiency. However, the removal efficiency decreased with increasing initial MB concentration. This is shown in Figure 11, where the percentage of MB removed decreases as the initial concentration increases from 5 mg/L to 20 mg/L. The lower removal efficiency at higher dye concentrations may be due to the saturation of the adsorption sites on the nanoparticle surface. As the dye concentration increases, more dye molecules are present in the solution, but the available adsorption sites on the nanoparticles remain constant. This results in a lower number of dye molecules adsorbed per unit surface area of the adsorbent, which reduces the overall adsorption capacity. In addition, the higher the dye concentration, the stronger the competition for the active sites, which further limits the number of dye molecules that can be effectively removed from the solution. At low initial concentrations, there are more free active sites on the adsorbent surface, which allows a higher proportion of dye molecules to interact with the adsorbent. As a result, the removal efficiency is higher. However, as the initial MB concentration increases, the available active sites on the nanoparticle surface are occupied more quickly, which reduces the adsorption capacity. These results highlight the importance of adsorbent dosage and initial dye concentration in optimizing the adsorption process for efficient dye removal in wastewater treatment applications.

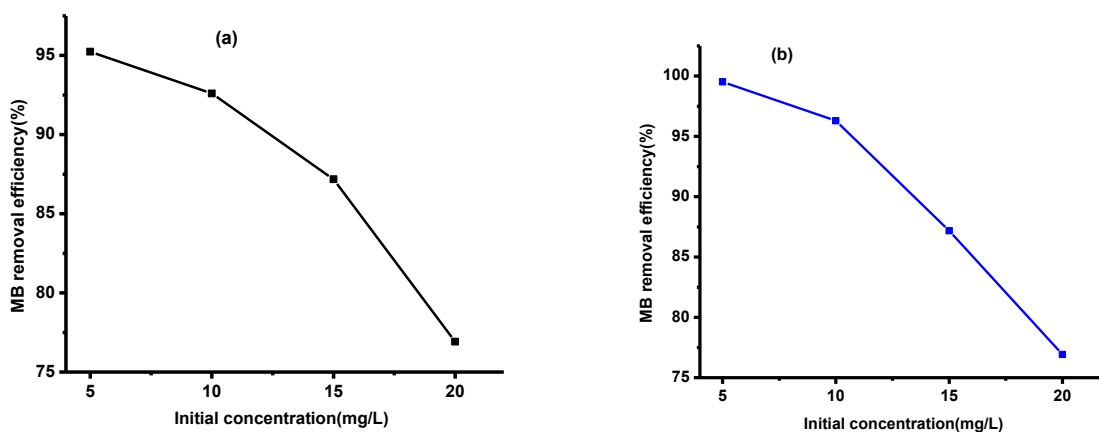


Figure 11: Effect of initial concentration on MB dye removal by (a) ZnO NPs, & (b) Fe-ZnO NPs

4.3.5 Reusability test of Fe doped ZnO NPs

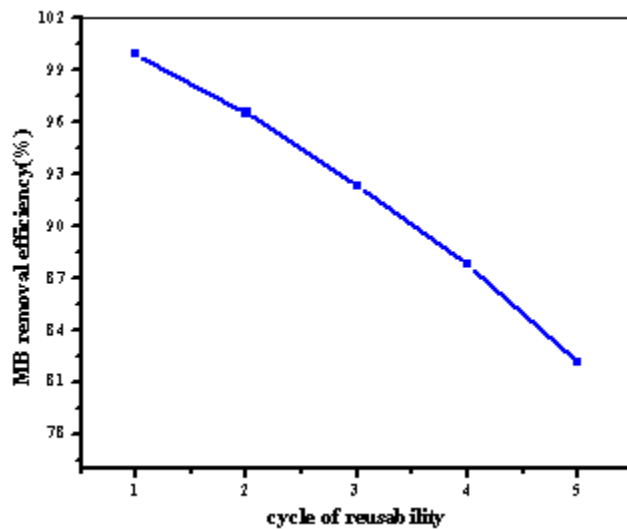
A key characteristic of an effective adsorbent is its ability to exhibit both high adsorption and desorption efficiency, enabling its reuse over multiple cycles without significant performance loss. In this study, the feasibility of reusing Fe-ZnO NPs composite for removal of methylene blue (MB) dye from aqueous solution was evaluated. The adsorption efficiency was tested at pH 9, contact time 45 min, and initial MB concentration 5 mg/L. The results presented in Figure 12 show that the Fe-ZnO NPs composite maintains high adsorption capacity even after multiple cycles of adsorption and desorption.

In the first cycle, the adsorption efficiency was an impressive 99.52%, indicating that the Fe-doped ZnO nanoparticles are highly effective at removing the dye from solution. However, as the adsorption and desorption cycles continued, a slight decrease in efficiency was observed. The adsorption efficiency dropped to 96.52% in the second cycle, 92.32% in the third cycle, 87.78% in the fourth cycle, and 82.10% in the fifth cycle. Despite this gradual reduction in efficiency, the nano composites still retained more than 80% of its original adsorption capacity even after five cycles of use. This suggests that Fe-ZnO NPs can function as a stable, effective, and eco-friendly adsorbent for wastewater treatment applications, capable of removing MB dye efficiently over multiple cycles without a significant decline in performance.

The ability of the Fe-ZnO NPs composite to maintain high adsorption efficiency over several cycles is crucial for its practical application in sustainable waste water treatment. The composite's regenerability and reusability are particularly important, as they reduce the overall cost of the

treatment process and minimize the need for new adsorbent materials after each cycle. Furthermore, the stability of the nano composite after repeated use indicates that it can be a reliable material for long-term environmental applications, contributing to more sustainable methods for removing toxic dyes and pollutants from industrial wastewater.

In general, the high adsorption and desorption efficiency of Fe-ZnO NPs makes them an excellent choice for reusable adsorbents in dye removal applications, with the potential for sustained effectiveness even after multiple cycles of use [65]. This suggests that Fe-ZnO NPs can function as a stable, effective, and eco-friendly adsorbent for wastewater treatment applications, capable of removing MB dye efficiently over multiple cycles without a significant decline in performance.



4.5 Adsorption kinetics Study

In adsorption studies, understanding the kinetics of dye removal is crucial for determining the efficiency and mechanism of the adsorption process. A variety of kinetic models can be employed to analyze the mass transfer and the rate at which methylene blue (MB) is transferred from the liquid phase to the surface of the adsorbent. In this study, the adsorption behavior of MB on to three different adsorbents, namely un-doped ZnO, Fe-doped ZnO, and other synthesized materials, was investigated using two commonly used kinetic models: the pseudo-first-order and pseudo-second-order models.

Pseudo-First-Order Kinetic Model

The pseudo-first-order kinetic model proposed by Lagergren (1898) is based on the assumption that the adsorption rate is proportional to the difference in adsorbate concentration at a given time. This model assumes that the adsorption rate follows a first-order response to sorbate concentration. The linear form of the pseudo-first-order model is expressed by the following equation:

$$\ln(q_e - q_t) = \ln q_e - k_1 t \dots \dots \dots Eq5$$

Here, q_e and q_t are the adsorption capacities (mg/g) at equilibrium and time t , respectively, and k_1 (min⁻¹) and k_2 (gmg⁻¹ min⁻¹) are the corresponding rate constants. This model is often used to describe adsorption processes where the rate of change in the amount of adsorbed dye with time is proportional to the difference between the equilibrium concentration and the instantaneous concentration.

Pseudo-Second-Order Kinetic Model

The pseudo-second-order kinetic model developed by Ho and McKay (1999) assumes that the adsorption rate is proportional to the square of the difference between the amount of dye adsorbed at time Δ and equilibrium. This model is commonly used to describe adsorption systems that may involve chemical adsorption or chemical bonding, assuming that the adsorption rate depends on the accessibility of the active site to the adsorbate. The linear form of the pseudo-second-order model is expressed as follows:

$$\frac{t}{qt} = + \frac{1}{k_2 q_e^2} + \frac{t}{q_e} \dots \dots \dots Eq6$$

the pseudo-second-order model is often used when adsorption follows a chemisorptions process, where the rate of adsorption depends on the availability of free sites and is influenced by the interactions between the adsorbate molecules and the adsorbent surface.

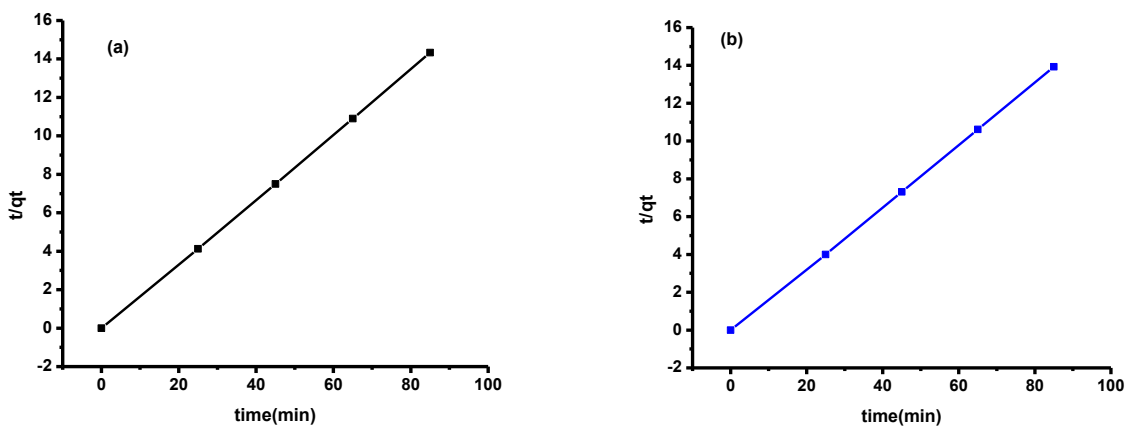
4.4.1 Pseudo-first order kinetics

The values of q_e , k_1 , k_2 and R^2 are collected in Table 3 and Fig. 13 shows the linear curves generated using the pseudo-first-order and pseudo-second-order kinetic models. The pseudo-first-order kinetic model was used to evaluate the adsorption kinetics of M on ZnO and Fe-ZnONP. The experimental data ZnO $q_{exp}(6.12)$, $q_{cal}(0.003)$ and Fe-ZnONPs $q_{exp}(7.04)$, $q_{cal}(0.09)$ do not form a favorable model due to the inconsistency and the fact that the correlation coefficient R^2 is not close to 1. As shown in Table 3, the adsorption of M on the head adsorbent [66].

4.4.2 Pseudo-second order kinetics

The mechanism of adsorption kinetics is described using the pseudo-second-order kinetic model over the entire contact time range. Compared with the pseudo-first-order model, the adsorption capacity q_{cal} (6.02 mg/g) calculated from the pseudo-second-order model is closer to q_{exp} (6.12 mg/g) and q_{cal} (6.95 mg/g) for ZnO NPs. It is also closer to k (7.04 mg/g) for Fe-ZnO NPs adsorbents as listed in Table 3. Additionally, the comparison of the two kinetic correlation coefficients (R^2) demonstrates that the pseudo-second-order model better describes the adsorption process of MB from aqueous solution. The R^2 value approaches 1 when the pseudo-second-order kinetic model (0.999 and 0.999) is compared with the pseudo-first-order kinetic model (0.454 and 0.572) for ZnO and Fe-ZnO NPs, respectively. As shown in Table 3 below, the generated pseudo-second-order kinetic model has higher correlation coefficient values than the pseudo-first-order kinetic model, indicating a closer agreement with the experimental adsorption data than the pseudo-second-order kinetic model. [66]

Figure13:pseudosecond-ordermodelsof(a)ZnO NPs, (b) Fe-ZnO NPs. Comparison of Kinetic Models:



By fitting the two kinetic models to the experimental data, the adsorption mechanism and the rate-limiting step of the process can be determined. A good fit to the pseudo-second-order model generally suggests that MB adsorption is dominated by chemical adsorption involving bond formation between dye molecules and active sites on the parent adsorbent surface. In contrast, a good fit to the pseudo-first-order model suggests a simpler physical adsorption mechanism in which the adsorption rate is largely dependent on concentration gradients rather than chemical bonds. The results obtained from fitting the data to both models allow researchers to calculate parameters such as the rate constants k_1 and k_2 , and to evaluate the correlation coefficients (R^2) to determine which model best represents the experimental data. A higher correlation coefficient (R^2) value for the pseudo-second-order model typically indicates that the adsorption process is predominantly controlled by chemisorptions or surface reaction rather than simple physical adsorption. In general, the application of the pseudo-first-order and pseudo-second-order kinetic models provides valuable insights into the adsorption mechanism of MB dye on the synthesized adsorbents, helping to determine the rate and nature of the adsorption process, as well as optimize conditions for maximum adsorption efficiency.

Table 3: Parameters of pseudo-1st order and pseudo-2nd order for synthesized samples

	ZnO NPs		Fe-ZnO NPs	
	Pseudo-1 st order	Pseudo 2 nd - order	Pseudo -1 st order	Pseudo-2 nd order
<i>qe</i> (experimental)	6.12	6.12	7.04	7.04
<i>qe</i> (calculated)	0.003	6.02	0.0967	6.95
K	0.00021	-0.421	-0.00071	-0.4721
R ²	0.454	0.999	0.572	0.999

The data presented in Table 3 shows the parameters derived from the pseudo-first-order and pseudo-second-order kinetic models for the adsorption of methylene blue (MB) dye on to ZnO NPs and Fe-ZnO NPs. The key parameters in the table include the experimental adsorption capacity *qe* (in mg/g), the calculated adsorption capacity (*qe* calculated from the respective kinetic model), the rate constant (*k*) for each model, and the correlation coefficient (*R*²).

Analysis of ZnO NPs

For ZnO NPs, the experimental equilibrium adsorption capacity (*qe*) is 6.12mg/g for the pseudo-first-order and 6.12 mg/g for the pseudo-second-order model, suggesting that the experimental values for both models are the same. However, the calculated values for each model are quite different. The pseudo-first-order model yields a very low calculated *qe* of 0.003 mg/g, which is much smaller than the experimental value. This indicates a poor fit of the first-order model to the data. On the other hand, the pseudo-second-order model shows a much more accurate calculated value of 6.02 mg/g, which is very close to the experimental value of 6.12 mg/g, suggesting that the adsorption process follows a pseudo-second-order kinetic model more closely. The rate constant of the pseudo-first-order model (δ) is very small (0.00021), which further indicates that this model does not accurately describe the head adsorption kinetics. In contrast, the rate constant of the pseudo-second-order model ($\delta = -0.421$) is much more significant, which reflects a better fit to the data and suggests that the head adsorption rate is controlled by a second-order process, including chemisorption. The correlation coefficient (δ^2) of the pseudo-first-order model is 0.454, which is a fairly low value, indicating a poor fit of the data to the model. In contrast, the pseudo-second-order model has a very high value of δ^2 (0.999), which suggests that the pseudo-second-order model provides an excellent fit to the experimental data and that the head adsorption process is dominated by a second-order mechanism.

Fe-ZnONP Analysis For Fe-ZnONP, the experimental equilibrium adsorption capacity (q_{∞}) is 7.04 mg/g for both the pseudo-first-order and pseudo-second-order models, which is again identical. The calculated values for the two models show a significant contrast. The pseudo-first-order model gives a calculated value of q_{∞} 0.0967 mg/g, which is much smaller than the experimental value, indicating a poor fit of this model. However, the pseudo-second-order model gives a calculated value of 6.95 mg/g, which is very close to the experimental value of 7.04 mg/g. This indicates that the adsorption process is better described by the second-order model. The rate constant (k_1) of the pseudo-first-order model is -0.00071, which is very small, further confirming the poor fit of this model. In comparison, the rate constant of the pseudo-second-order model ($k_2=0.4721$) is more significant, indicating a significant adsorption rate consistent with the second-order kinetic model. The correlation coefficient of the pseudo-first-order model is 0.572, which is relatively low and further confirms that this model does not adequately describe the adsorption kinetics. However, the pseudo-second-order model shows a perfect fit with a R^2 value of 0.999, further supporting the idea that the adsorption process follows the second-order kinetic model for Fe-ZnO nanoparticles. Overall, the data suggest that the adsorption of methylene blue (MB) dye on both ZnO and Fe-ZnO nanoparticles is better described by the pseudo-second-order kinetic model. The low correlation coefficients and poor fit to the pseudo-first-order model for both adsorbents indicate that the adsorption process is not controlled by a simple first-order mechanism. The high values of R^2 for the pseudo-second-order model (close to 1 for both adsorbents) suggest that the release or formation of chemical bonds between the head sorbate (MB dye) and the head adsorbents (ZnO or Fe-ZnO nanoparticles) is the dominant mechanism controlling the process adsorption. Furthermore, the adsorption capacities calculated from the pseudo-second-order model are in good agreement with the experimental values, which further validates the second-order kinetic model to explain the dye adsorption on both ZnO and Fe-ZnO nanoparticles

CHAPTER FIVE

5. CONCLUSION AND RECOMMENDATION

5.1 Conclusion

In this study, the adsorption of methylene blue (MB), a widely used synthetic dye and model pollutant, was investigated using zinc oxide (ZnO) and iron-doped zinc oxide (Fe-doped ZnO) nanoparticles. The objectives were to examine how these nanoparticles behave under various operating conditions and to evaluate their potential as adsorbents for the removal of toxic dyes from aqueous solutions. To achieve this, the synthesized adsorbents were characterized using several analytical techniques, including X-ray diffraction (XRD), Fourier transform infrared (FTIR) spectroscopy, and ultraviolet-visible (UV-VIS) spectroscopy. ZnO and Fe-doped ZnO nanoparticles were synthesized and detailed structural and optical analyses were performed. The XRD patterns showed that both ZnO and Fe-doped ZnO particles exhibited the hexagonal wurtzite structure characteristic of ZnO.

The diffraction peaks were sharp, indicating the high crystallinity and purity of the phase. The presence of well-defined peaks indicates that the nanoparticles are well formed and have a consistent crystal structure. This structural perfection is very important for efficient adsorption of contaminants, as the surface properties play a crucial role in the interaction with the dye molecules. The average particle size of the nanoparticles was calculated using X-ray diffraction analysis. The results showed that the average particle size of pure ZnO nanoparticles was about 24 nm, while the iron-doped ZnO nanoparticles showed a slightly smaller average particle size of 20 nm. The smaller particle size of the iron-doped ZnO could be attributed to the influence of iron ions during the synthesis process, which facilitates better nucleation and thus produces finer nanoparticles. Smaller nanoparticles generally have a larger surface area, which can enhance the adsorption efficiency.

The FTIR spectroscopy spectrum of the nanoparticles showed various absorption peaks, which helped in identifying the functional groups present on the nanoparticle surface. The spectrum indicates the presence of hydroxyl groups (-OH), which are typical of metal oxide surfaces. In addition, functional groups such as flavonoids, alkaloids, and tannins derived from plant extracts were identified, confirming the role of plant extracts in stabilizing the nanoparticles. These organic functional groups are important in enhancing the stability of the nanoparticles and may contribute to the overall dye removal process through additional interactions with dye molecules. UV-vis analysis showed significant changes in the absorption spectra of iron-doped ZnO nanoparticles compared to pure ZnO. The absorption peak of pure ZnO occurred in the

UV region, which is typical of ZnO nanoparticles due to their wide band gap. However, the absorption spectra of Fe-doped ZnO nanoparticles shifted toward the visible range, indicating that the band gap was narrowed due to Fe doping. This change in absorption wavelength suggests that Fe-doped ZnO nanoparticles may be more effective under visible light, which is important for practical applications where UV light is not always available. The adsorption efficiency of the nanoparticles for methylene blue dye removal was tested under various operating conditions. Several factors were optimized to determine the best conditions for maximum dye removal.

5.2 Recommendation

Based on the findings of this study, several recommendations can be made for further research and potential applications of Fe-doped ZnO nanoparticles in environmental remediation, particularly in the removal of toxic dyes like methylene blue from wastewater:

Further Optimization of Synthesis Conditions: While the synthesis conditions for Fe-doped ZnO nanoparticles in this study were optimized for methylene blue dye removal, further research can explore the influence of additional synthesis parameters, such as temperature, precursor concentration, and iron doping levels.

Study of Other Pollutants: Although methylene blue was used as the model pollutant in this study, it is essential to assess the adsorption efficiency of Fe-doped ZnO nanoparticles for a wider range of industrial pollutants, such as organic dyes, heavy metals, and pharmaceutical contaminants. Testing the versatility of Fe-doped ZnO as a biosorbent in removing various contaminants from wastewater would provide a more comprehensive understanding of its potential for broad environmental applications. Comparative studies between different types of metal oxide

Nano particles (e.g. Fe-doped ZnO vs Fe-doped TiO₂, or ZnO vs. CuO) could also provide valuable insights into optimizing adsorbent selection. **Scale-Up and Pilot Studies:** While this study demonstrated promising results in the laboratory, scaling up the synthesis process and conducting pilot-scale studies will be essential for assessing the practicality of using Fe-doped ZnO nanoparticles in real-world wastewater treatment. These studies should focus on evaluating the performance of the nanoparticles under varying environmental conditions, such as different temperatures, pH levels, and complex water matrices (e.g. presence of salts, competing ions, or organic matter). Additionally pilot studies can provide important data on the economic feasibility and technical challenges associated with large-scale applications

REFERENCES

1. G. Ren, H. Han, Y. Wang, S. Liu, J. Zhao, X. Meng and Z. Li, Recent advances of photocatalytic application in water treatment: A review, *Nanomaterials* 11(7) (2021) 1804. <https://doi.org/10.3390/nano11071804>
2. C. Regmi, B. Joshi, S.K. Ray, G. Gyawali, R.P. Pandey, Understanding Mechanism of Photocatalytic Microbial Decontamination of Environmental Wastewater, *Frontiers in Chemistry* 6 (2018) 33. <https://doi.org/10.3389/fchem.2018.00033>
3. Zhang, F., Wang, X., Liu, H., Liu, C., Wan, Y., Long, Y., Cai, Z., 2019. Recent advances and applications of semiconductor photocatalytic technology. *Appl. Sci.* 9 (12), 2489. <https://doi.org/10.3390/app9122489>.
4. Adedokun, O., Bello, I.T., Sanusi, Y.K., Awodugba, A.O., 2020. Effect of precipitating agents on the performance of ZnO nanoparticles based photo-anodes in dyesensitized solar cells. *Surf. Interfaces* 21, 100656. <https://doi.org/10.1016/j.surfin.2020.100656>.
5. Karuppaiah, S., Annamalai, R., Muthuraj, A., Kesavan, S., Palani, R., Ponnusamy, S., Nagarajan, E.R., Meenakshisundaram, S., 2019. Efficient photocatalytic degradation of ciprofloxacin and bisphenol A under visible light using Gd₂WO₆ loaded ZnO/ bentonite nanocomposite. *Appl. Surf. Sci.* 481, 1109–1119. <https://doi.org/10.1016/j.apsusc.2019.03.178>
6. Kareem, M.A., Bello, I.T., Shittu, H.A., Awodele, M.K., Adedokun, O., Sanusi, Y.K., 2020. Green synthesis of silver nanoparticles (AgNPs) for optical and photocatalytic applications: A review. *IOP Conf. Ser.: Mater. Sci. Eng.* 805 (1), 012020. <https://doi.org/10.1088/1757-899X/805/1/012020>
7. Anand, V., Srivastava, V.C., 2015. Zinc oxide nanoparticles synthesis by electrochemical method: Optimization of parameters for maximization of productivity and characterization. *J. Alloys Compd.* 636, 288–292. <https://doi.org/10.1016/j.jallcom.2015.02.189>.
8. Lang, J., Wang, J., Zhang, Q.i., Li, X., Han, Q., Wei, M., Sui, Y., Wang, D., Yang, J., 2016. Chemical precipitation synthesis and significant enhancement in photocatalytic activity of Ce-doped ZnO nanoparticles. *Ceram. Int.* 42 (12), 14175–14181. <https://doi.org/10.1016/j.ceramint.2016.06.042>.

9. A. Ayele, D. Getachew, M. Kamaraj and A. Suresh, Phycoremediation of synthetic dyes: An effective and eco-Friendly algal technology for the dye abatement, *Journal of Chemistry* (2021) 9923643. <https://doi.org/10.1155/2021/9923643>.
10. Y. Kayabaşı, Methylene blue and its importance in medicine, *Demiroglu Science University Florence Nightingale Journal of Medicine* 6 (2020) 136–145. <https://doi.org/10.5606/fng.btd.2020.25035>.
11. N. Kaur, J. Kaushal, P. Mahajan and A.L. Srivastav, Design of hydroponic system for screening of ornamental plant species for removal of synthetic dyes using phytoremediation approach, (2022). <https://doi.org/10.21203/rs.3.rs-1301660/v1>.
12. Guarín, J. R., Moreno-Pirajan, J. C., &Giraldo, L. (2018). Kinetic Study of the Bioadsorption of Methylene Blue on the Surface of the Biomass Obtained from the Algae *D. Antarctica*. *Journal of Chemistry*, 2018, 1 to12. <https://doi.org/10.1155/2018/2124845>.
13. Wang, ZL: Zinc oxide nanostructures: growth properties and applications. *J.Phys. Condens. Matter.*, 2004; 16: 829–858.
14. AshaRani PV, Low KahMun G, Hande MP, Valiyaveetil S. 2009. Cytotoxicity and genotoxicity of silver nanoparticles in human cells. *ACS Nano*. 3:279–290. doi:10.1021/nn800596w.
15. Khan ZUH, Sadiq HM, Shah NS, Khan AU, Muhammad N, Hassan SU, Tahir K, safi SZ, Khan FU, Imran M, et al. 2019. Greener synthesis of zinc oxide nanoparticles using *Trianthemaportulacastrum* extract and evaluation of its photocatalytic and biological applications. *J PhotochemPhotobiol*. 193:147–157. doi:10.1016/j.jphotobiol.2019.01.013
16. Kumar SS, Venkateswarlu P, Rao VR, Rao GN. 2013. Synthesis, characterization and optical properties of zinc oxide nanoparticles. *Int Nano Lett*. 3(1):30. doi:10.1186/2228-5326-3-30.
17. Osmond MJ, Mccall MJ. 2010. Zinc oxide nanoparticles in modern sunscreens: an analysis of potential exposure and hazard. *Nanotoxicology*. 4:15–41. doi:10.3109/17435390903502028
18. Yadav A, Prasad V, Kathe AA, Raj S, Yadav D, Sundaramoorthy C, Vigneshwaran N. 2006. Functional finishing in cotton fabrics using zinc oxide nanoparticles. *Bull Mater Sci*. 29:641–645. doi:10.1007/s12034006-0017-y

19. Kołodziejczak-Radzimska A, Jesionowski T. 2014. Zinc oxide—from synthesis to application: a review. *Materials*. 7 (4):2833–2881. doi:10.3390/ma7042833
20. Hariharan C. 2006. Photocatalytic degradation of organic contaminants in water by ZnO nanoparticles: revisited. *ApplCatal A Gen*. 304:55–61. doi:10.1016/j.apcata.2006.02.020.
21. J. H. Tian, J. Hu, S. S. Li, F. Zhang, J. Liu, J. Shi, X. Li, Z. Q. Tian and Y. Chen, Improved seedless hydrothermal synthesis of dense and ultralong ZnO nanowires, *Nanotechnology* 22, 245601 (9pages) (2011).
22. Kumar A, Ram J, Samarth RM, Kumar M (2005). Modulatory influence of *Adhatoda vasica* Nees leaf extract against gamma irradiation in Swiss albino mice. *Phytomedicine*, 12: 285-293.
23. Yinebeb Tariku (2008). In vitro efficacy study of some selected Medicinal plants against *Leishmania* spp. MSc. thesis in Medicinal Chemistry, Addis Ababa University, Addis Ababa, Ethiopia.
24. EndalewAmenu (2007). Use and management of medicinal plants by indigenous people of Ejaji area (Chelyaworeda) West Shoa, Ethiopia: An ethnobotanical approach. MSc. thesis in Dryland Biodiversity, Addis Ababa University, Addis Ababa, Ethiopia.
25. TilahunTeklehaymanot and MirutseGiday (2007). Ethnobotanical study of medicinal plants used by people in Zegie Peninsula, Northwestern Ethiopia. *Journal of Ethnobiology and Ethnomedicine* 3:12.
26. Haile Yineger, EnsermuKelbessa, Tamrat Bekele and ErmiasLulekal (2008). Plants used in traditional management of human ailments at Bale Mountains National Park, Southeastern Ethiopia . *Journal of Medicinal Plants Research* 2(6):132-153.
27. Moa Megersa (2010). Ethnobotanical study of medicinal plants in WayuTukaWereda, East Wollega Zone of Oromia Region, Ethiopia. MSc. thesis in Biology (Botanical Science), Addis Ababa University, Addis Ababa, Ethiopia.
28. Pathak RP (1970). *Therapeutic Guide to Ayurvedic Medicine (A handbook on Ayurvedic medicine)* Shri Ramdayal Joshi Memorial Ayurvedic Research Institute, 1: 121.
29. A. Janotti and C. G. Van de Walle, Fundamentals of zinc oxide as a semiconductor, *Rep. Prog. Phys.* 72, 126501 (29pages) (2009).

30. Ü. Özgür, Ya. I. Alivov, C. Liu, A. Teke, M. A. Reshchikov, S. Doan, V. Avrutin, S. J. Cho, and H. Morkoç, A comprehensive review of ZnO materials and devices, *Journal of Applied Physics* 98, 041301 (2005).
31. C. Liu, F. Yun, H. Morkoc, Ferromagnetism of ZnO and GaN: A review, *Journal of Materials Science: Materials in Electronics* 16, 555-597 (2005).
32. S. J. Pearton, D. P. Norton, M. P. Ivill, A. F. Hebard, J. M. Zavada, W. M. Chen, and I. A. Bunyanova, Ferromagnetism in transition-metal doped ZnO, *Journal of Electronic Materials* 36, No. 4, 462-471 (2007).
33. A. B. Djuricic, and Y. H. Leung, Optical properties of ZnO nanostructures, *Small* 2, No. 8-9, 944-961 (2006).
34. J. Cui, Zinc oxide nanowires, *Materials Characterization* 64, 43-52 (2012).
35. H. Morkoc and U. Ozgur, General properties of ZnO, *Zinc Oxide: Fundamentals, materials and device technology*, WILEY-VCH Verlag (2009) p.1-2.
36. Z. Fan and J. G. Lu, Zinc Oxide Nanostructures: Synthesis and properties, *J. NanosciNanotechnol.* 5, 1561-73 (2005).
37. C. Klingshirn, ZnO: From basics towards applications, *Phys. Stat. Sol. (b)* 244 No. 9, 3027-3073 (2007).
38. H. Morkoç and U. Özgur, *Zinc Oxide: Fundamentals, materials and device technology*, WILEY-VCH Verlag GmbH & Co. KGaA, Weinheim (2009) p.284-287.
39. H. Ohno, Making nonmagnetic semiconductors ferromagnetic, *Science* 281, 951-956 (1998).
40. D. Karmakar, S. K. Mandal, R. M. Kadam, P. L. Paulose, A. K. Rajarajan, T. K. Nath, A. K. Das, I. Dasgupta, and G. P. Das, Ferromagnetism in Fe-doped ZnO nanocrystals: Experiment and theory, *Physical Review B* 75, 144404 (2007).

41. J. M. D. Coey, M. Venkatesan and C. B. Fitzgerald, Donor impurity band exchange in dilute ferromagnetic oxides, *Nature Materials* 4, 173-179 (2005).
42. Mirzaei, A., Chen, Z., Haghghat, F. and Yerushalmi, L. (2018) Hierarchical magnetic petal-like Fe₃O₄-ZnO@gC₃N₄ for removal of sulfamethoxazole, suppression of photocorrosion, by-products identification and toxicity assessment. *Chemosphere* 205, 463-474.
43. Elmolla, E.S. and Chaudhuri, M. (2010) Degradation of amoxicillin, ampicillin and cloxacillin antibiotics in aqueous solution by the UV/ZnO photocatalytic process. *Journal of hazardous materials* 173(1), 445-449
44. Gaya, U.I. and Abdullah, A.H. (2008) Heterogeneous photocatalytic degradation of organic contaminants over titanium dioxide: A review of fundamentals, progress and problems. *Journal of Photochemistry and Photobiology C: Photochemistry Reviews* 9(1), 1-12.
45. Takata, T. and Domen, K. (2009) Defect Engineering of Photocatalysts by Doping of Aliovalent Metal Cations for Efficient Water Splitting. *The Journal of Physical Chemistry C* 113(45), 19386-19388.
46. Moosvi, S.K., Majid, K., & Ara, T. (2017). Study of thermal, electrical, and photocatalytic activity of iron complex doped polypyrrole and polythiophene nanocomposites. *Industrial & Engineering Chemistry Research*, 56(15), 4245-4257.
47. Ahmad, J., & Majid, K. (2018). Enhanced visible light driven photocatalytic activity of CdO-graphene oxide heterostructures for the degradation of organic pollutants. *New Journal of Chemistry*, 42(5), 3246-3259.
48. RekhaPachaiappan, SaravananRajendran, GomathiRamalingam (2021). Green Synthesis of Zinc Oxide Nanoparticles by Justicia adhatoda Leaves and Their Antimicrobial Activity
49. Karaghool, H. A. K. (2021). Biodecolorization of methylene blue using aspergillus consortium. *IOP Conference Series: Earth and Environmental Science*, 779(1), 012111. <https://doi.org/10.1088/1755-1315/779/1/012111>.
50. TadesseBirhanu and DerejeAbera (2015). Survey of ethno-veterinary medicinal plants at selected HorroGudurru District, Western Ethiopia. *African Journal of Plant Science* 9(3): 185-192.
51. K.A. Isai and V.S. Shrivastava, Photocatalytic degradation of methylene blue using ZnO and 2%Fe-ZnO semiconductor nanomaterials synthesized by sol-gel method: a

- comparative study, SN Applied Sciences 1 (2019) 1247. <https://doi.org/10.1007/s42452-019-1279-5>.
52. R.P. Pal Singh, I.S. Hudiara and S.B. Rana, Effect of calcination temperature on the structural, optical and magnetic properties of pure and Fe-doped ZnO nanoparticles, Materials Science- Poland 34 (2016) 451–459. <https://doi.org/10.1515/msp-2016-0059>.
53. Banu, K. S. & Cathrine, L. 2015. General techniques involved in phytochemical analysis. International Journal of Advanced Research in Chemical Science, 2, 25-32.
54. Mamo, B. Y., & Zeleke, T. D. (2022). Green synthesis of rGO/Ag nanocomposite using extracts of Cinnamomum verum plant bark: Characterization and evaluation of its application for Methylene blue dye removal from aqueous solutions. *International Journal of Nano Dimension*, 13(4), 414-434.
55. Cahino, A.M., et al., *Characterization and evaluation of ZnO/CuO catalyst in the degradation of methylene blue using solar radiation*. Ceramics International, 2019. **45**(11): p. 13628-13636.
56. M.M. Ba-Abbad, A.A.H. Kadhum, A.B. Mohamad, M.S. Takriff, K. Sopian, Chemosphere 91 (11) (2013) 1604–1611.
57. R. Ashraf, S. Riaz, Z.N. Kayani, S. Naseem, Mater. Today Proc. 2 (10) (2015) 5384–5389.
58. S. Hameed, A.T. Khalil, M. Ali, M. Numan, S. Khamlich, Z.K. Shinwari, M. Maaza, Nanomedicine 14 (6) (2019) 655–673.
59. F. Naz, K. Saeed, Inorg. Nano-Met. Chem. 51 (1) (2021) 1–11.
60. Jamdagni, P., P. Khatri, and J. Rana, *Green synthesis of zinc oxide nanoparticles using flower extract of Nyctanthes arbor-tristis and their antifungal activity*. Journal of King Saud University-Science, 2018. **30**(2): p. 168-175
61. Sofowora, A. (1996). Research on medicinal plants and traditional medicine in Africa. *The Journal of Alternative and Complementary Medicine*, 2(3), 365–372. <https://doi.org/10.1089/acm.1996.2.365>
62. Das, S. K., Khan, M. M., Parandhaman, T., Laffir, F., Guha, A. K., Sekaran, G., & Mandal, A. B. (2013). Nano-silica fabricated with silver nanoparticles: Antifouling adsorbent for efficient dye removal, effective water disinfection and biofouling control. *Nanoscale*, 5(12), 5549. <https://doi.org/10.1039/c3nr00856h>
63. Wu, Q., Feng, C., Wang, C., & Wang, Z. (2013). A facile one-pot solvothermal method to produce superparamagnetic graphene–Fe₃O₄ nanocomposite and its application in the

- removal of dye from aqueous solution. *Colloids and Surfaces B: Biointerfaces*, 101, 210–214. <https://doi.org/10.1016/j.colsurfb.2012.05.036>
64. Elmorsi, T. M. (2011). Equilibrium isotherms and kinetic studies of removal of methylene blue dye by adsorption onto Miswak leaves as a natural adsorbent. *Journal of Environmental Protection*, 02(06), 817–827. <https://doi.org/10.4236/jep.2011.2609>
65. Sun, H., Cao, L., & Lu, L. (2011). Magnetite/reduced graphene oxide nanocomposites: One step solvothermal synthesis and use as a novel platform for removal of dye pollutants. *Nano Research*, 4(6), 550–562. <https://doi.org/10.1007/s12274-011-0111-3>
66. Kavithad, D., & Namasivayam, C. (2007). Experimental and kinetic studies on methylene blue adsorption by Coir Pith Carbon. *Bioresource Technology*, 98(1), 14–21. <https://doi.org/10.1016/j.biortech.2005.12.008>

APPENDIX



Figure 1: Synthesis of Nanoparticles

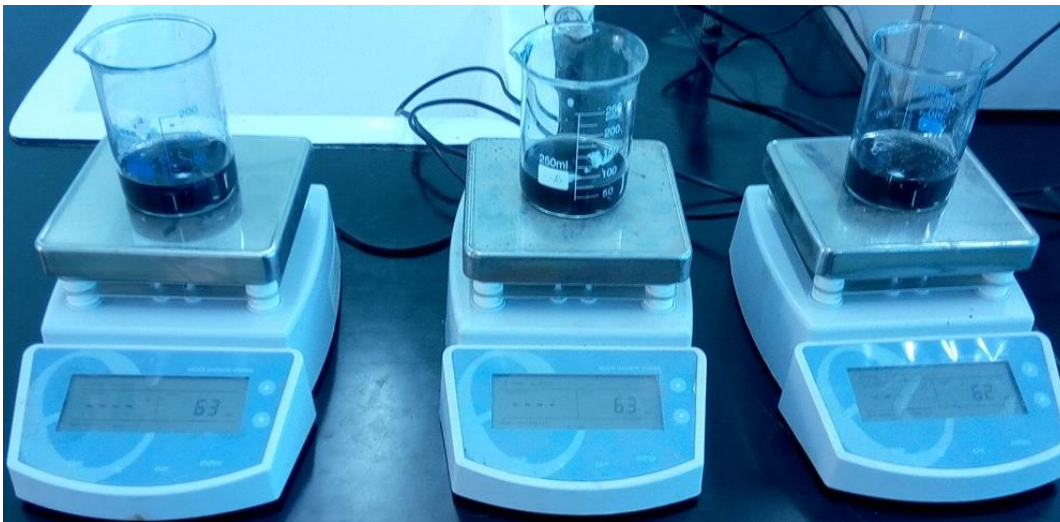


Figure 2: adsorption experiment stirring by digital magnetic stirrer



Figure 3: Filtration process in adsorption experiment

